Kajetan Heigert, B.Sc.

Speicherverhalten und Abflussdynamik aktiver Blockgletscher am Beispiel Ölgrube Süd, Kaunertal.

MASTERARBEIT

zur Erlangung des akademischen Grades

Master of Science

Masterstudium Erdwissenschaften

eingereicht an der

Technischen Universität Graz

Betreuer

Ass.-Prof. Mag. Dr.rer.nat., Gerfried Winkler

Institut für Erdwissenschaften

Graz, August 2018

EIDESSTATTLICHE ERKLÄRUNG

Ich erkläre an Eides statt, dass ich die vorliegende Arbeit selbstständig verfasst, andere als die angegebenen Quellen/Hilfsmittel nicht benutzt, und die den benutzten Quellen wörtlich und inhaltlich entnommenen Stellen als solche kenntlich gemacht habe. Das in TUGRAZonline hochgeladene Textdokument ist mit der vorliegenden Masterarbeit identisch.

Datum

Unterschrift

Danksagung

Ich möchte mich hiermit bei allen bedanken, die mich in meinem Studium und speziell während der Entstehung der Masterarbeit unterstützt haben.

Ein großes Dankeschön geht an meinen Betreuer Gerfried Winkler für die immer unkomplizierte und konstruktive Unterstützung der Masterarbeit.

Ebenso gilt mein Dank Rita Pleschberger und speziell Thomas Wagner, für die Hilfe bei den vielen spontanen Fragen die bei der Ausarbeitung der Masterarbeit entstanden sind.

Danke an Karl Krainer für das Überlassen der vielen Daten die diese Masterarbeit erst so möglich gemacht haben.

Zu guter Letzt danke ich meinen bisher noch ungenannten Helfern im Feld, Georg Erharter, Marcus Eder und Michael Popp.

Abstract

While general research on rock glaciers got a fair amount of attention during the last two decades, the hydro(geo)logy of rock glaciers is a rather unknown field. Recent studies show that (relict) rock glacier are likely to play a vital part as water sheds in alpine environments. Despite rising temperatures active rock glaciers can still be found in large numbers in Austria, a thorough understanding of their discharge dynamics has yet to be developed.

At the area of investigation in Kaunertal (Tyrol) at Ölgrube Süd rock glacier hydrogeological measurements are done for more than 10 years. In the course of this thesis data series with runoff measurements, electrical conductivity and weather data from 2014 to 2017 is evaluated and presented. The data is supplemented by 96 Isotope samples taken in 2017 at the rock glacier springs and in the catchment area.

The hydrograph shows pronounced seasonal and daily variations mainly induced by the weather. Peak discharge is reached during the snow melting period in early summer where values of more than 500 l/s are common. After the winter snow cover has melted in late summer and further towards the winter, the variations decrease. Eventually a several months long base flow stadium (approx. 10 l/s) is observed, lasting until the next melting season.

Master recession curve analysis suggests a heterogeneous aquifer structure. Characterized by highly conductive preferential flow paths who quickly discharge strong precipitation and slower permeable layer(s) who form a yearlong unfrozen storage. The estimated groundwater volume stored in ÖGS rock glacier is about 0.6 $x10^6$ m^3.

The duality of the Aquifer is confirmed by the investigation of the electric conductivity of water. “Event-water” passes the rock glacier in an average of approx. 4,5 hours after the maximum groundwater recharge. It becomes apparent that already the water infiltrating the rock glacier has very variable electric conductivities from approx. 1 µS/cm to 500 µS/cm.

The analysis of stable water isotopes as well as the electric conductivity suggest that different waters are mixed in the rock glacier and most likely rock glacier ice is melted.Tracer tests with break through times of a few hours align with the concept of a heterogeneous rock glacier structure. This indicates that retention capabilities are limited in case of strong groundwater recharge.

Kurzfassung

Während die Forschung an Blockgletschern in den letzten beiden Jahrzehnten einige Aufmerksamkeit erfahren hat, ist die Hydro(geo)logie von Blockgletschern ein relativ unerforschtes Thema. Aktuelle Untersuchungen an reliktischen Blockgletschern zeigen, dass diesen wahrscheinlich eine bedeutende Rolle in den alpinen Einzugsgebieten zukommt. Trotz steigender Temperaturen gibt es in Österreich noch eine große Anzahl an aktiven Blockgletschern, ein umfassendes Verständnis ihrer Abflussdynamik muss zunächst noch entwickelt werden.

Im Arbeitsgebiet am Ölgrube Süd Blockgletscher im Kaunertal werden bereits seit über 10 Jahren hydrogeologische Messungen und Untersuchungen durchgeführt. Im Zuge dieser Arbeit werden Abflussmessungen, elektrische Leitfähigkeit und Wetterdaten von 2014 bis 2017 ausgewertet und präsentiert. Ergänzt werden diese durch 96 Isotopenproben die an den 3 Hauptquellen und im Einzugsgebiet genommen wurden.

Die Ganglinie zeigt deutliche saisonale und tägliche Schwankungen die maßgeblich vom Wetter verursacht werden. Spitzenabflusswerte von mehr als 500 l/s werden üblicherweise zur Schneeschmelze im Frühsommer erreicht. Nachdem die Winterschneedecke zum Spätsommer und Winter geschmolzen ist, verringert sich die Variabilität. Schließlich wird in ein mehrere Monate langes Stadium des Basisabflusses (ca. 10 l/s) beobachtet welches bis zur nächsten Schneeschmelze anhält.

Die Analyse der „Master recession curve“ deutet auf einen heterogenen Aquifer Aufbau hin. Charakterisiert durch sehr gut leitenden bevorzugte Fließwege mit denen starke Niederschläge rasch abgeleitet werden und langsamer durchlässige Schichten die einen ganzjährig ungefrorenen Speicher bilden. Das ermittelte Grundwasserspeichervolumen des ÖGS Blockgletschers beträgt ungefähr 0.6 $x10^6$ m^3.

Diese Dualität des Aquifers wird von den Untersuchungen der elektrischen Leitfähigkeit des Wassers bestätigt. „Event-Wasser“ passiert den Blockgletscher durchschnittlich innerhalb von etwa 4,5 Stunden nach der maximalen Grundwasserneubildung. Es zeigt sich, dass bereits das in den Blockgletscher infiltrierende Wasser sehr unterschiedliche elektrische Leitfähigkeiten von ca. 1 µS/cm bis 500 µS/cm besitzt.

Die Analyse der stabilen Wasserisotope deuten wie die elektrische Leitfähigkeit darauf hin, dass im Blockgletscher eine Durchmischung von verschiedener Wässer stattfindet und wahrscheinlich Blockgletschereis abgeschmolzen wird. Tracer Versuche mit Durchbrüchen von wenigen Stunden fügen sich ebenfalls in das Modell des heterogenen Blockgletscheraufbaus. All dies deutet darauf hin, dass die Rückhaltefähigkeiten im Fall von starker Grundwasserneubildung begrenzt sind.

Content:

1 Introduction

In the last decades awareness about the effects of worldwide climate change has developed to one of the major topics in the modern society. In the course of this global phenomenon the research on climate related topics gained a new significance. The development of alpine permafrost is one of them.

Rock glaciers are one of the most visible forms of alpine permafrost, the rock glacier inventory for Tirol (Austria) alone includes 3145 rock glaciers who cover 167,2 km^2 which is equivalent to about 1,3 % of Tirol (Krainer, et al., 2012).

Another climate change related topic is the evolution of the hydrological cycle in the alps. Following Barnett (2005) currently the alps hydrological cycle is dominated by melting snow and ice, but the increasing temperatures are expected to cause less winter precipitation in form of snow and an earlier snowmelt in spring, leading to a shift of the regions runoff peaks into late winter and early spring while summers will be especially dry. As the alps are vastly supplying the main rivers in Europe, changes in the alpine watersheds have a direct impact on our water supply and ecosystems (Winkler, et al., 2016).

As suggested by Clow (2003) talus slopes and rock glaciers form a detention reservoir for event precipitation, furthermore the mostly rock glacier internal permafrost ice forms a second substantial groundwater reservoir in alpine regions. Developing this thought takes rock glaciers from “simple” indicators of permafrost to environmentally and economically important groundwater storages.

While the relict rock glacier Schöneben was and is researched in detail to serve as a reference project for the impact of a relict rock glacier on alpine runoff (Winkler, et al., 2016), the active rock glacier Ölgrube Süd could serve as the counterpart of an active, ice bearing, rock glacier.

While most of the recent studies on ÖGS RG focused on its dynamic, ice content, structure and overall geology and geomorphology (Krainer, et al., 2000, 2006; Berger, et al., 2004; Hausmann, et al. 2012; Rieder, 2017), two specific studies on the hydrology of active rock glaciers, with some data of ÖGS RG set the baseline. Krainer et al. (2002) show that discharge of active rock glaciers in the Austrian Alps is to a large extent controlled by local weather conditions. The discharge is dominated by strong seasonal and daily variations with maxima caused during peak snowmelt in early summer, thus active rock glaciers discharge resembles the one of glaciers. The use of stable isotopes and electric conductivity allowed a further characterization of the discharge of active rock glaciers. In Krainer et al. (2007), the authors demonstrate that the high discharge at the beginning of the melting season is originated in melting snow and ice, thus towards the winter the share of groundwater on the overall runoff increases. Also, the seasonal trend can be interrupted by precipitation events, a significant part of event water passes through the rock glacier in only a few hours.

The aim of this thesis is to get an even better understanding of the hydrodynamics of an active rock glacier, with a special regard to storage capabilities and groundwater components.

The topic and interrogation arose from the project “Water resources management issues of rock glaciers in alpine catchments of the Eastern Alps – storage capacity, flow dynamics and hydrochemistry in particular heavy metal pollution (RG-HeavyMetal) funded by the Ministry of Sustainability and Tourism and the federal governments of Styria, Tyrol, Salzburg, Carinthia and Vorarlberg headed by Gerfried Winkler at the KFU Graz.

2 Basics

2.1 Rock glaciers

Definition:

Following Barschs (1996) widely used definition, rock glaciers are lobar- to tongue shaped bodies consisting of frozen, unconsolidated material, supersaturated with interstitial icecement and ice lenses, who creep downwards as a result of gravity and internal deformation of the ice. While not wrong, this definition is mostly valid for so called active rock glaciers.

Genesis and structure:

Rock glaciers are one of the most visible forms of alpine permafrost due to their striking morphology (Krainer, et al., 2012). In the Austrian alps rock glaciers are mostly a few hundred meters long with a width of 100 to 200 m, individual rock glaciers with length up to 1,5 km are known (Krainer, et al., 2009).

The genesis of rock glaciers is a discussed topic, a short roundup can be found in Nyenhuis (2005). Two established concepts of a periglacial development of a rock glacier are shown in Figure 1:

A) Debris derived rock glaciers – the glacier located in the background of the rock glacier advances and deposes moraine material in the root zone of the rock glacier. Melting water of the glacier can refreeze in the debris material filling the pore volume of these sediments, forming the root zone of a new rock glacier (Hughes, et al., 2003).

B) Talus derived rock glaciers – are located beneath talus slopes where avalanches and rock falls accumulate. Ice can be built up by the transformation of avalanche snow or intruding melting water. This way an ice content of more than 60 % can be reached which can result in gravitational movement (Hughes, et al., 2003; Nyenhuis, 2005).

Furthermore, rock glaciers can be developed from debris covered glaciers as shown by Krainer and Mostler (2000).

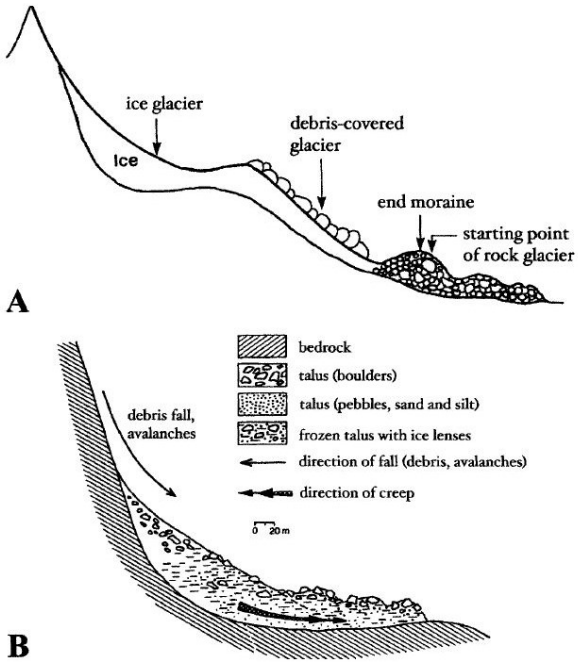

Figure 1: Two concepts for the formation of rock glaciers: A) debris derived rock glacier, B) talus derived rock glacier. Illustration by Hughes et al., (2003) modified of Barsch (1996).

Classification:

Rock glaciers can be distinguished into three different types, mainly with respect to ice content and velocity as displayed in Figure 2: a) active rock glaciers, b) inactive rock glaciers and c) relict rock glaciers (Krainer, et al., 2009), usually with a development in this order.

Active rock glaciers (Figure 2 a)) are characterized by sharp borders, a back shaped by trenches and ridges and a steep front of about 40 to 45° being the result of the ongoing gravitational movement. Active rock glaciers show little to no vegetation and a fresh front (Krainer, 2015). The rate of movement is usually in the range of decimeters but can reach up to several meters a year (Krainer, et al., 2006). Beneath a protective "active layer" of blocky material their core holds an ice content of 40 to 60 % (Hausmann, et al., 2012; Krainer, et al. 2015). At the front face of an active rock glacier one or more springs can be found whose water temperature is constantly below 1 °C all year long (Krainer, et al., 2009). Geophysical studies on active rock glaciers suggest, that beneath the rock glaciers ice core an unfrozen sediment layer composes the contact zone to the bedrock (Hausmann, et al., 2012; Krainer, et al. 2015).

Inactive rock glaciers (Figure 2 b)) can be distinguished from active rock glaciers by their non existing movement, i.e. a velocity of less than 1 cm/a (Barsch, 1996). They are further divided into "climatic inactive", where despite still carrying ice, estimates state about 10 to 15 % (Krainer, et al., 2012), ice content is too low to support further movement, and "dynamic inactive" where the reason for the stationarity may be the lack of debris at the root zone or that the rock glacier reaches a flatter topography where gravitational movement is obstructed (Krainer, 2015). Due to missing movement vegetation can start to conquer the inactive rock glaciers surface and depending on the ice loss, collapse structures may develop (Nyenhuis, 2005)

Rock glaciers without an ice core are called relict rock glaciers (Figure 2 c)), the cores melting created a volume loss which caused collapse structures visible on the back on the rock glacier. As the relict rock glacier shows no movement and developed out of an active rock glacier via the inactive rock glacier, erosion took place for a longer period so that the edges are less sharp, the fronts gradient is less pronounced and the surface area is vegetated (Nyenhuis, 2005).

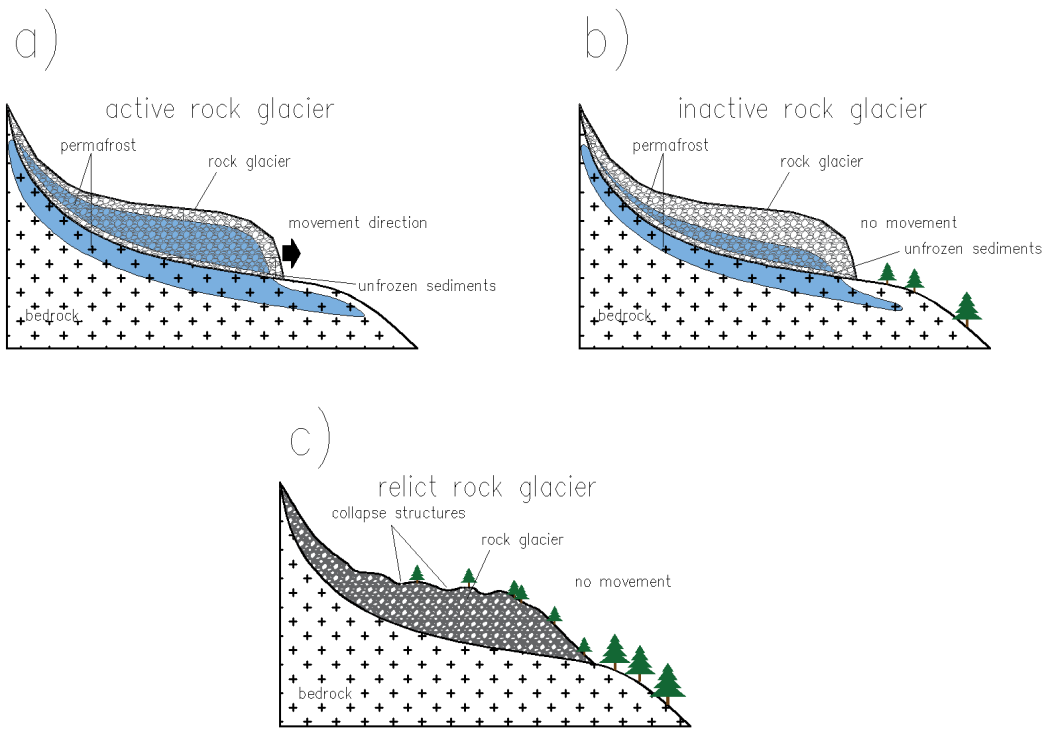

Figure 2: Three types of rock glaciers: active, inactive and relict. The main distinction is made by the ice content. Modified after Pauritsch (2016).

Hydrogeology of rock glaciers:

Research on the hydrology of rock glaciers is still a developing field. Due to the heterogeneity of rock glaciers and their respective local environmental conditions still no superordinate understanding has been established. Studies on the hydrology/hydrogeology of rock glaciers are usually aligned with the rock glacier classification of active-/inactive- and relict rock glaciers, in view of the ice content. In the following the key points of rock glacier hydrogeology are condensed:

Active and inactive rock glaciers can be summarized when regarding their hydrogeology, since both types have an ice core. Compared to relict rock glaciers, the main difference concerning the hydrogeology of active and inactive rock glaciers is the additional internal ice content. Due to the debris cover this ice is shielded from warmer temperatures resulting in decelerated melting rates compared to glaciers (Krainer, et al., 2009). Generally, discharge of active rock glaciers is characterized by pronounced seasonal and daily variations mainly controlled by the weather conditions. During the early summer the melting of snow and ice usually leads to the annual discharge maximum as studies of discharge vs. $\delta^{18}O$ and EC show (Krainer, et al., 2002, 2007). During fair weather periods runoff shows pronounced daily variations of the discharge. After the winter snow cover has melted the discharge gradually decreases and EC as well as $\delta^{18}O$ records suggest that the groundwater and ice-melt contribution to discharge rises (Krainer, et al., 2002, 2007; Engel, et al. 2016). This descending trend can be interrupted by rainfall events that cause sharp peaks in discharge. Yet data shows that these event waters pass through the rock glacier within a few hours after precipitation (Krainer, et al., 2007; Rieder, 2017). Extensive studies on relict rock glacier “Schöneben” in the Seckauer Tauern in Styria (Austria) summarized in Winkler et al. (2016) show a comparable discharge dynamic. Shortly after a precipitation event the discharge rises, natural tracer records suggest that event water is barely stored. It is shown that this rock glacier has a heterogeneous internal structure leading to a multi stage

discharge behavior comparable to karst aquifers. Coarse grained layers allow a fast pathway for infiltrating water while a fine grained base layer decelerates the flow and leads to a delayed discharge.

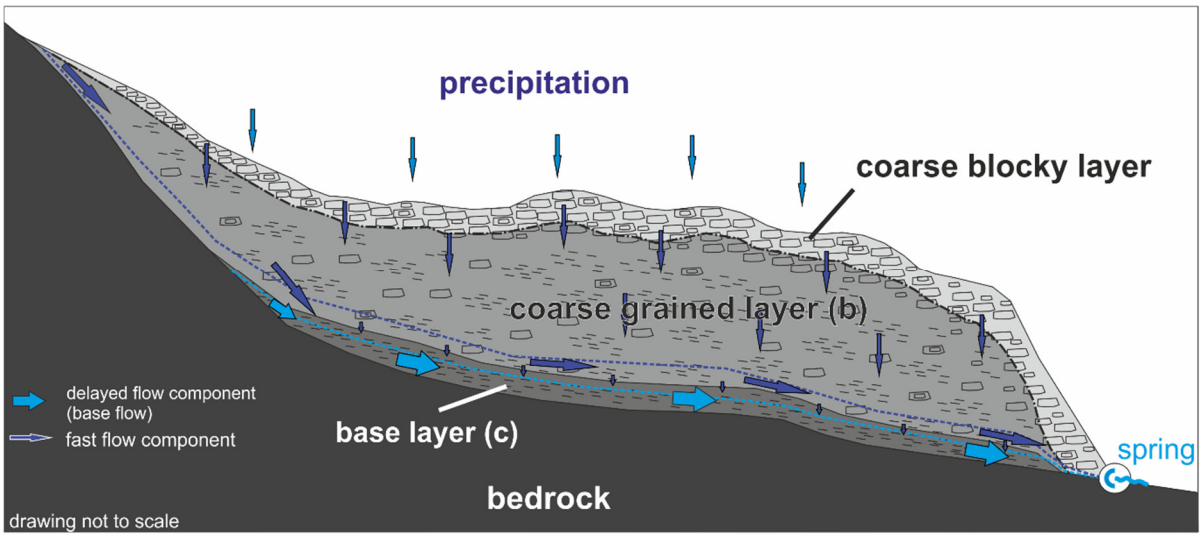

Figure 3: Conceptual model of the relict Schöneben rock glacier with a layered structure (Winkler, et al., 2016).

2.2 Geographical framework

Subject of investigation (Figure 4) in this thesis is the active rock glacier “Ölgrube Süd” (OGS), located in a hanging valley called “Innere Ölgrube”, 29 km SSE of the town Landeck in the upper Kaunertal valley, which is a part of the Ötztal Alps in Tyrol (Austria).

The base of the catchment area is at about 2340 m above sea level, the vertical difference to the highest peak of the area Hintere Ölgrubenspitze with 3293 m is 953 meters. The investigation area is surrounded by steep rock cliffs and slopes from north beyond east to south. Towards the west, the hanging valley steeply declines into the about 400 m deeper main valley Kaunertal.

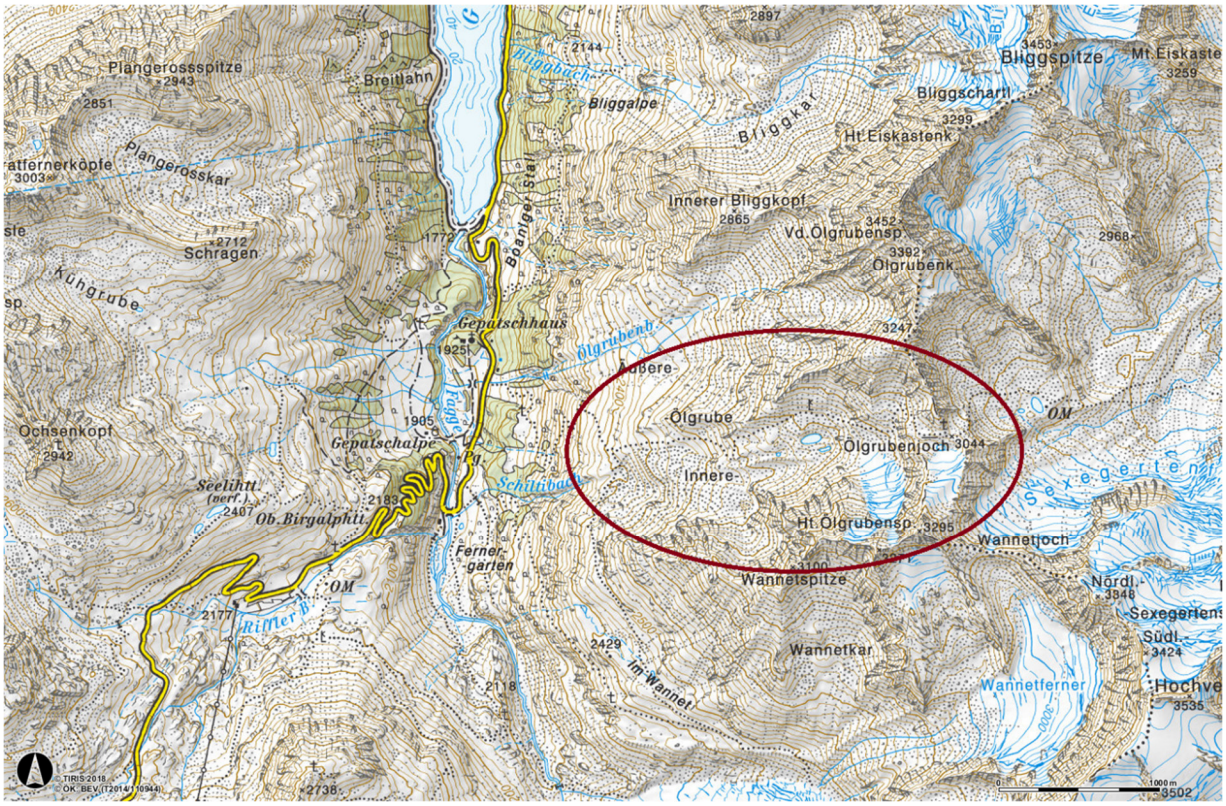

Figure 4: Area of investigation in the upper Kaunertal (Ötztal Alps, Tirol).

2.3 Geology and geomorphology

Geologically the area of research is located in the Ötztal-Stubai-Komplex (ÖSK), it consists of various metamorphic rocks and is part of the Oberostalpin (Schmid, et al., 2004). In the catchment area the bedrock is set up by orthogneiss, paragneiss and mica schist (Hoinkes, et al., 1993). The bedrock is overlain by different quaternary sediment types with variable thickness. At the foot of steep walls talus slopes, mainly consisting of blocky material, stones and gravel, accumulate. The valley bottom is filled with moraine material including grain sizes from silt to blocks (Figure 5) (Rieder, 2017).

The area is characterized by the active rock glacier “Ölgrube Süd”, it consists of two separate tongues (Figure 6), whereby the northern one clearly excels the southern in length, width and height. Together they form a 880 m long and 250 m wide rock glacier with a front height of up to 70 m and a slope angle of 40° to 45° (Krainer, 2015). Beside the rock glacier the area contains several lateral moraines dated back to the last glacial highstand of 1850, the corresponding glacier “Hinterer Ölgrubenferner” has since then withdrawn to its present position (Berger, et al., 2004). The glaciers mouth is at an elevation of approximately 2800 m (a.s.l.), where a small glacial stream appears leading into the first of two ponds at the base of a rock ledge. The two ponds are located in ground moraine material forming a small depression, no surface outlet is visible so that a significant infiltration into the moraine material is assumed. Further down a streamlet accumulates for some dozen meters before disappearing in the blocky rock glacier root zone (see Figure 5).

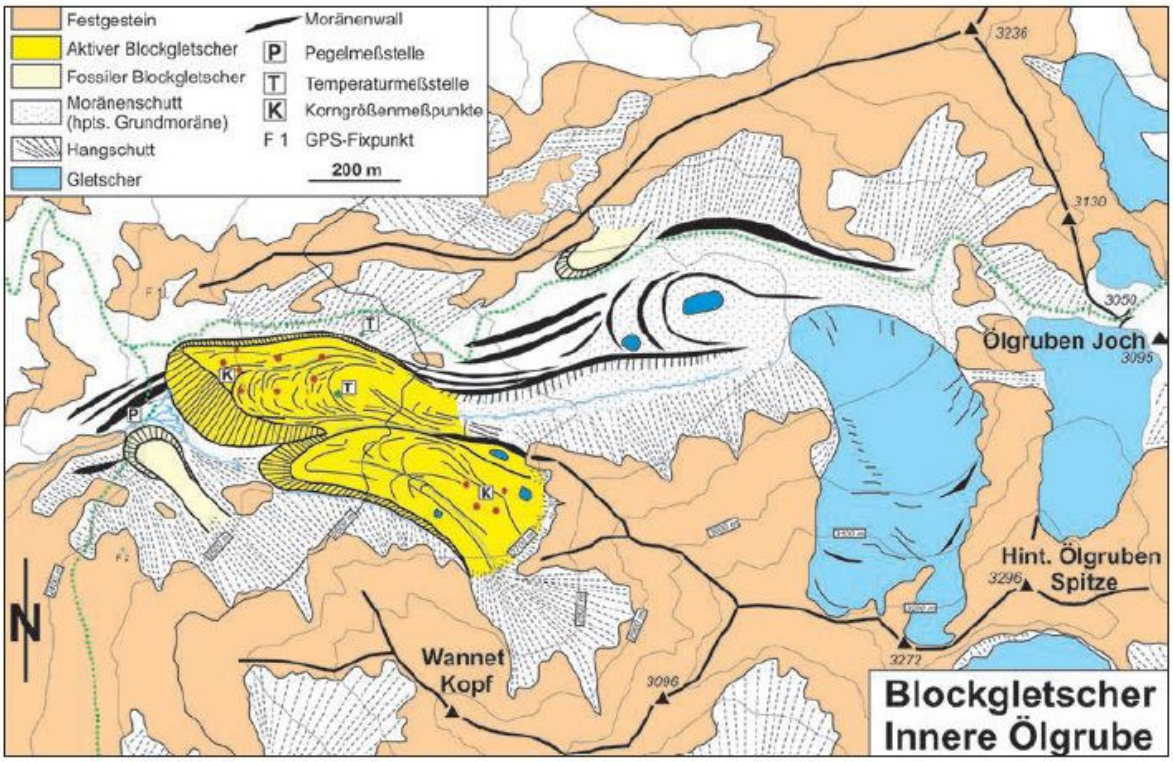

Figure 5: Geologic-geomorphological map of the rock glacier Ölgrube Süd (Krainer, 2015).

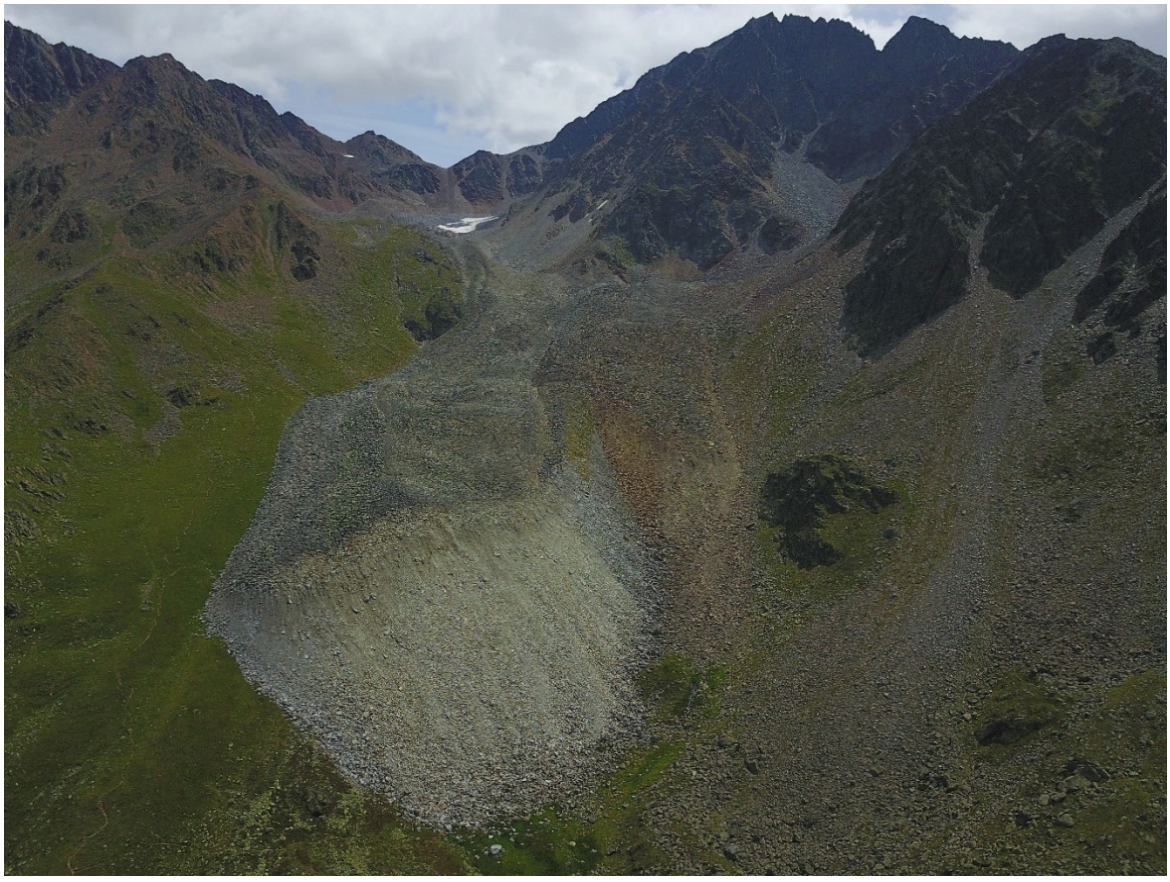

Figure 6: The active rock glacier Ölgrube Süd with its two tongues and the impressive front face. (Aerial Photo by Georg Erharter, July 2017)

2.4 Test site and data Set at Ölgrube Süd

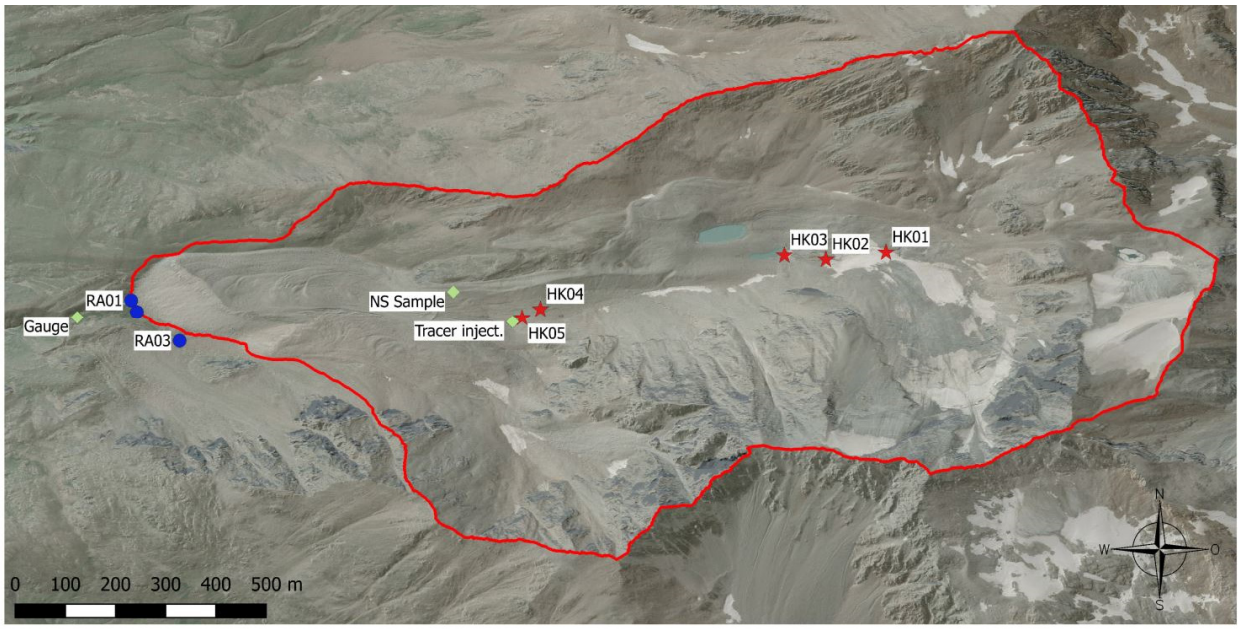

Figure 7: Aerial view of the research area with marked test sites. Catchment area (red frame) engulfs ca. 1,834 km². (tirisMaps, 2018)

As displayed in Figure 7 the sampling locations and test sites align along the flow path from the glacier Hinterer Ölgrubenferner (HK01) to the water gauge.

The data base used for the research was generated and collected in four field trips during summer of 2017 in the upper Kaunertal valley. Additionally, this dataset is supplemented by the work of previous studies in this area, mainly conducted by Aaron Rieder and supervised by Karl Krainer. All in all, the results of 94 water isotope samples, three years of discharge measurement, two uranine tracer tests, 6 salt tracer tests, water temperature, electric conductivity measurements and the matching weather data are incorporated into this study.

Using data loggers and automatic water sampling instruments the values for some of the physical parameters are available for long term time series, ranging from days up to years with resolutions up to a few minutes. Other measurements that were taken manually are only representative for a short time period when viewed without further data, but their implementation helps to paint the greater picture. A comprehensive view of the gathered data is given in Figure 8, where the different ways of data acquisition are shown in timelines. Only validated data is shown in this figure, solely the periods with usable records are displayed.

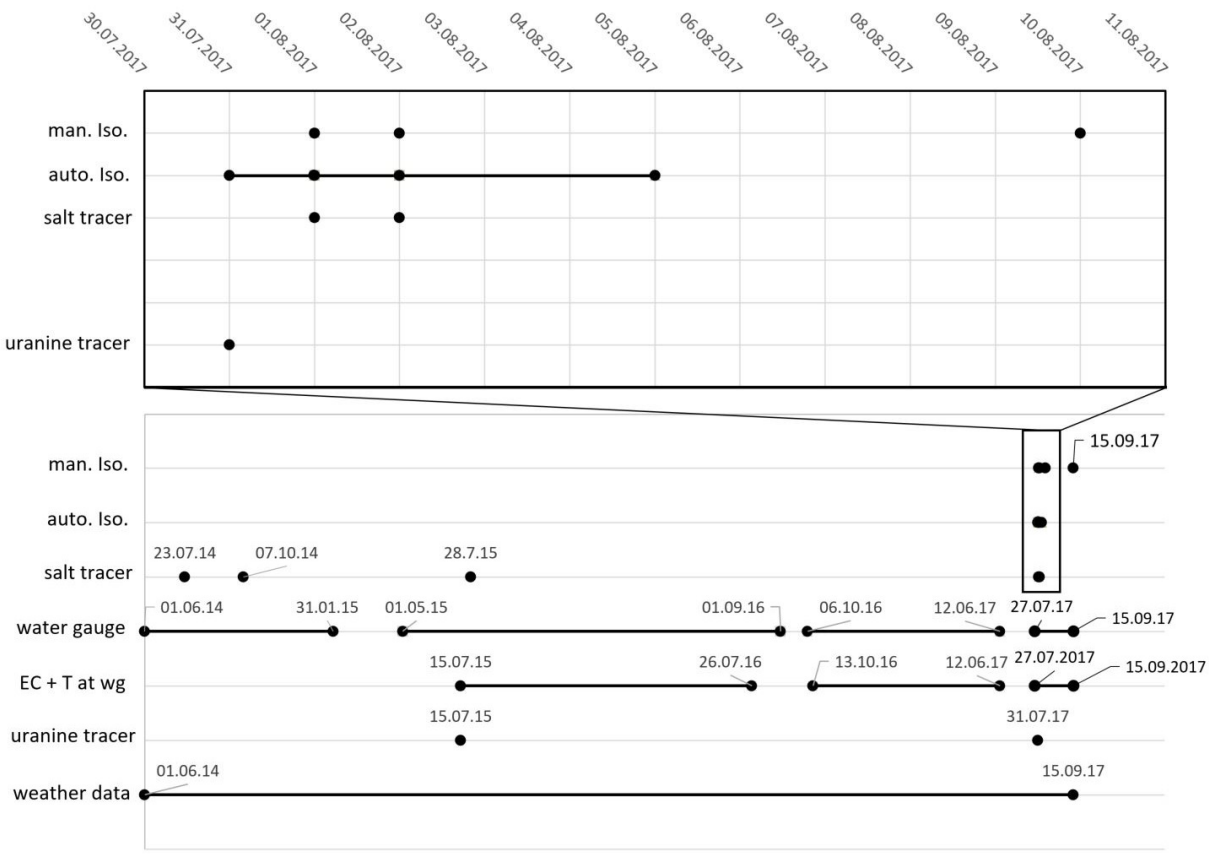

Figure 8: The timeline shows when and what kind of data was acquired before- and during the making of this masters thesis. The timelines show only periods where validated, usable data is present. Abbreviations: manually taken isotopic samples (man. Iso.), isotope samples taken with the automatic sampler (auto. Iso.), discharge measurements by the salt tracer method (salt tracer), water level at gauge (water gauge), measurement of electronic conductivity and water temperature at water gauge (EC+T and wg), uranine tracer test input (uranine tracer) and weather data at TIWAG station "Weißsee" (weather data).

Water gauge:

In a creek ("Schilt Bach") formed by the confluence of the three main springs of the RG, that most likely forms the major drainage for the RG ÖGS, a water gauge with two separate data loggers was installed by Karl Krainer. The data loggers are air pressure compensated and take hourly measurements of the hydraulic head (pressure), electric conductivity and temperature of the water.

Salt tracer tests:

Three salt tracer tests performed 2017 by the author supplement a multitude of discharge measurements from previous years.

Uranine tracer tests:

The results of two uranine tracer tests are displayed.

Isotope samples:

Two different sampling approaches have been used to gain isotopic data. The first approach was with the help of an automatic sampling device. Beginning in the afternoon of the 31.07.2018 at 16:13 o'clock it was set up to take samples in a 1 h interval for a time span of 48 h. On the 02.08.2018 at 12:09, the sampler was started to fill his 24 bottles in a 6 h interval. Due to malfunctions of the automatic sampling device only 54 samples were taken, some with questionable quality.

As a second method, several samples are taken manually at defined locations. The locations are shown in Figure 7, each sample is completed with an in-situ temperature and electric conductivity measurement. The sampling locations “HK” are set up to cover a rough elevation profile of the area in the catchment area of the rock glacier (springs). Aiming to identify possible height related differences in the isotopic composition and the general shares and properties of rainwater and meltwater that infiltrate the rock glacier. A single composite sample of the rainfall from 31.07.2018 to 15.09.2018 was gathered at a location lying roughly in the middle of the catchment area. Finally, the three main springs “RA” at the ÖGS rock glaciers front are sampled regularly to further characterize the overall system. All in all, 42 samples were manually taken from 31.07. to 02.08.2018 and on the 10.08.2018 and 15.09.2018.

Electric conductivity:

Measurements of electric conductivity (EC) were done with portable probes, mostly while taking water samples and at the water gauge, where the SEBA probe records the EC in an hourly interval.

Weather data:

Temperature and precipitation data are kindly provided by the “Tiroler Wasserkraft AG” (TIWAG) who operate a meteorological station in the upper Kaunertal near the ski resort “Kaunertaler-Gletscher” at 2464 m above sea level. Although the station is in about 4 km distance to the research area, the benefit of a yearlong highly resoluted weather record shall not be unused. With the help of an elevation correction factor of 0.5 °C per 100 m height (Kuhn, et al., 2013), the mean air temperature in the research area can be interpolated. Furthermore, the general weather situation is an important factor in the interpretation of the gathered runoff data since precipitation and melting periods of snow and permafrost ice affect the runoff dynamic of the ÖGS rock glacier.

3 Methods

To get a thorough knowledge of the hydrodynamic behavior of the active rock glacier ÖGS several tests, ranging from single sampling and measuring up to long term data logging, were deployed in the field. The combination of several methods emphasizes their strengths, compensates their weaknesses and contributes to the better understanding of a hydrogeological system.

3.1 Runoff Log / Hydrograph

Discharge measurement "Salt-Tracer Method":

The measurement of a discharge with the help of a tracer is a well-established method for creeks and streams with irregular shape and turbulent flow (e.g. Morgenschweis, 2010). The method using salt (Natriumchloride) as tracer is based on the direct measurement of electric conductivity, which is linked to the tracer concentration. Here a set of two probes "Tracersystem TQ-S" from the manufacturer "Sommer Messtechnik" was used. The probes were calibrated in-situ with a defined calibration solution added stepwise into a defined volume of creek water to ensure correct measurements in the following salt tracer tests.

Before the actual measurements the necessary flow distance between the injection point of the tracer and the measuring point(s) is determined. It is important to ensure a complete mixing of the tracer in the stream. The distance can be calculated by a variety of empirical formulas that include parameters such as the present discharge, width of the stream and others (e.g. Morgenschweis, 2010). Due to the alpine terrain in this case, the possibilities for injection and measurement size are very limited and were chosen to ensure the most effective mixing possible.

A known amount of Natriumchloride is dissolved in a bucket of creek/stream water. About 50 m downstream of the injection site, two probes that continuously measure the electric conductivity at the left and right side of the stream. The electric conductivity is measured and recorded for a short time before the injection in order to get a baseline. After the instantaneous injection of the NaCl brine the electric conductivity is recorded until the baseline is reached again.

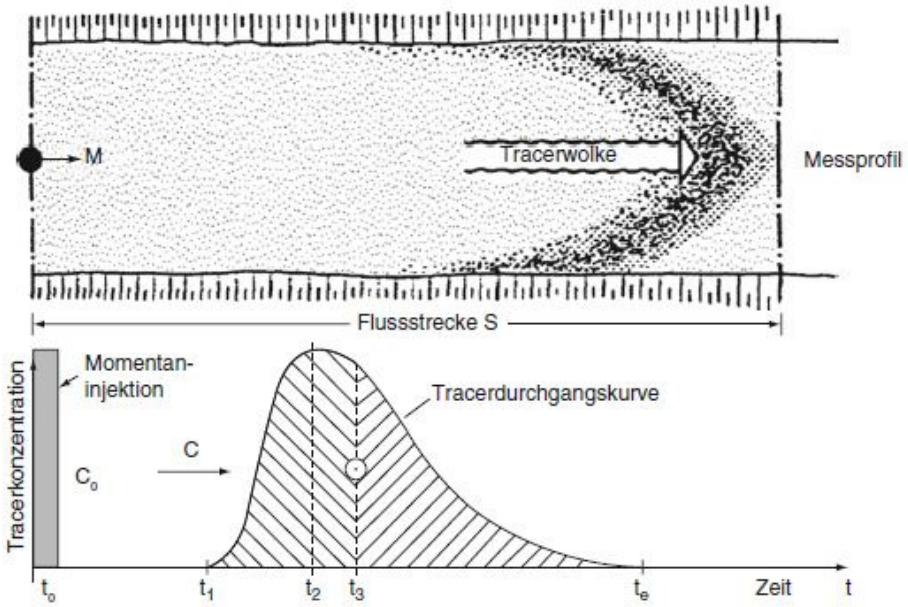

Figure 9: Principle of the "Integration Method", discharge measurement with a (salt) tracer (Morgenschweis, et al., 1991).

The recorded values are plotted in a time vs. conductivity (concentration) diagram and form a so called "breakthrough-curve", with a typical rapid ascent and a slightly delayed descend. The concentration is calculated via a calibration that is done before the main test. There, a defined amount of the creeks water is enriched with a buffer solution of distilled water and NaCl in several steps. A first rating curve is created to link the concentration and electric conductivity for the later determination of the discharge. With the premise of a constant discharge Q during the test, the discharge can be calculated following Equation 1. The value was automatically calculated by the probes associated software from "Sommer Messtechnik" and is the mean value of the two TQ-S probes that were used simultaneously in the creek during each test.

Equation 1: Calculation of discharge using the salt tracer method e.g. (Goldscheider, et al., 2007).

$$Q = \frac{M}{\int_0^t C - C_0 dt}$$	Q = Discharge [m^3/s] M = Amount of used tracer [g] C = Observed tracer concentration [g/m^3] C_0= background tracer concentration [g/m^3] t = time interval [s]

Rating curve to hydrograph:

As described in e.g. Morgenschweiss (2010), the pressure measurements of a data logger are transferable into indirect runoff measurements via a water level – runoff relation that can be established by a so called rating curve as shown in Figure 10.

The rating curve is used to calculate the real runoff Q [l/s] by linking the pressure data of the two loggers with actual discharge data. Due to the irregular shape of the creek it is not possible to calculate the runoff via a weir formula. Thus, the salt tracer method is applied to obtain several individual discharge values. To create a proper rating curve, it is preferable to cover a wide range of discharge values from the lowest to the highest water level over a time. This means that discharge measurements (the salt tracer test) must be done at different times and seasons to create a rating curve with extensive validity.

Various discharge measurements performed at different states of runoff are then linked to the according pressure measurements of the data logger. Then these pairs of values are used to fit a suitable function which can now be used to calculate a discharge value Q [l/s] from the related water level at all times.

A possible source of error to consider is: The link between the measured pressure and the discharge can only be drawn if a consistent profile is given, when at a certain water level new flow paths are activated that are not measured by the pressure gauge, the function cannot describe this behavior.

With the aim of achieving a realistic rating curve several discharge measurements by using the salt-tracer technique were performed over several years in different seasons.

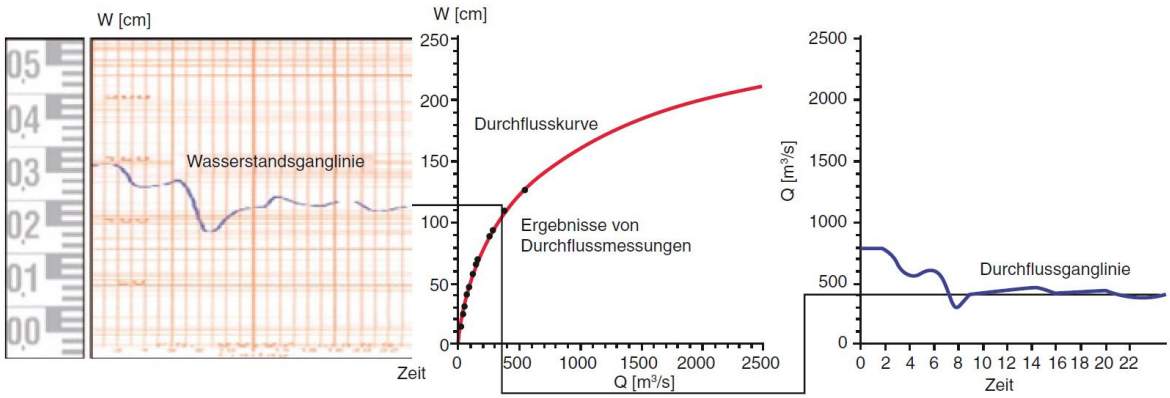

Figure 10: Establishing a water level - runoff relation (Wasserstand – Durchfluss) by fitting a rating curve (Durchflusskurve) to a broad range of individual runoff measurements (Morgenschweis, 2010).

3.2 Hydrograph analysis

Combining the rating curve with the loggers water level records, a time-discharge diagram can be set up. Thereby the discharge of the creek is monitored, depending on the time-resolution of the data short events as well as long time trends can be observed. A complete hydrograph is a crucial tool used to describe the hydrologic-systems behavior as it complements the other methods with discharge values. If the hydrograph shows the discharge over a long-time period, it is likely that all aspects of discharge behavior are recorded so it can be used to fully characterize the spring/creek.

Discharge variability, discharge quotient:

Variability in discharge is generally the result of precipitation- and infiltration conditions (Hölting, et al., 2013) and, with respect to rock glaciers, melting processes of permafrost ice. The discharge variability is evaluated by the "discharge quotient", the ratio of the lowest to highest measured runoff of a spring (Equation 2).

Equation 2: Calculation of discharge quotient (e.g. Hölting & Coldeway 2013).

$\frac{Q_{min}}{Q_{max}}$	Q_{min}: minimum measured discharge Q_{max}: maximum measured discharge

Hölting et al., (2013) state a ratio of 1/10 for karst springs and 7/10 for a spring originating of a sandy gravel aquifer. The value is an indication for the retention ability of a catchment area and the two examples can be considered as the extreme opposites.

Recession curve analysis, Maillet

For the hydrograph analysis a Master recession curve (MRC) was compiled. This was done using a Microsoft Excel VBA script by Posavec (2017). A MRC is constructed either manually or by software, where each recession segment of a hydrograph is first separated and then beaded in a time-runoff graph, depending on the peak discharge value at the beginning of this segment. The composite is then fitted with a model (MRC) which describes discharge behavior of a spring from maximum event runoff to final baseflow.

The recession curve, as shown in Figure 11, is that part of the hydrograph that starts after a local maximum which is normally generated by precipitation or melting events and ends right before the next ascent of the hydrograph. The whole range of discharge devolution can be seen in a recession curve resulting from long dry periods that followed a significant recharge event leading to undisturbed drainage of the just newly refilled aquifer storage.

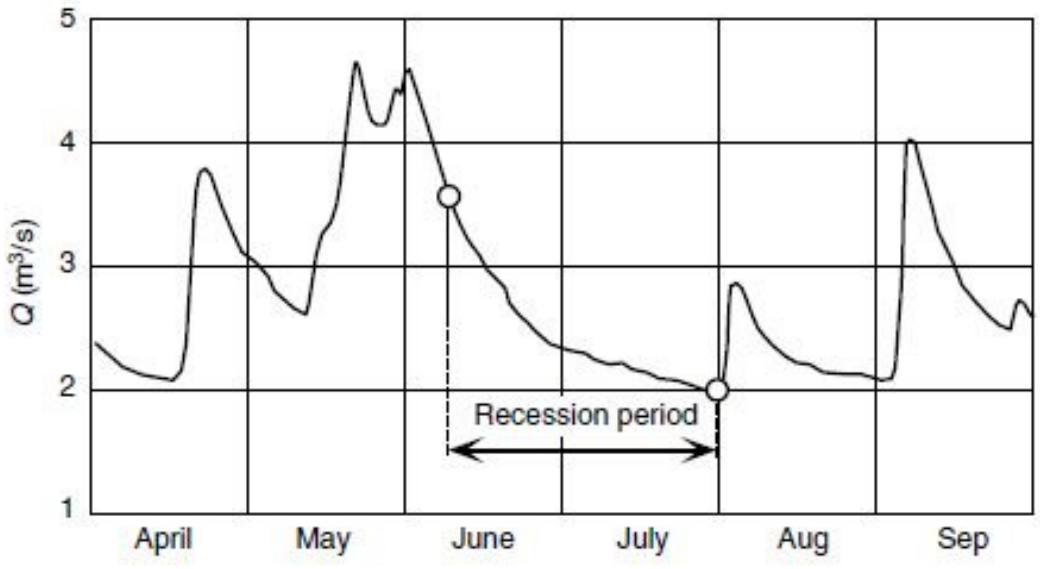

Figure 11: Exemplary recession curve for a segment of a hydrological year (Kresic, 2007).

The recession curve analysis was applied for the description of flow dynamics and storage capacity of (relict) rock glacier springs (e.g. Winkler, et al., 2016). It allows to put numbers to the development of discharge behavior making it comparable to other aquifer systems. Several mathematical models have been established for the recession curve analysis through the time, but despite its age and simplicity, the approach of Maillet (1905) is still one of the most frequently used (Dewandel, et al., 2003), its application is described in detail by e.g. Kresic (2007). The recession curve is based on the exponential Maillet formula (Equation 3) representing the concept of drainage of a linear store. Plotted in a semi-logarithmic time-discharge graph (Figure 12), the discharge curve is shown as a straight line which is adjusted to (a segment of) the recession curve as exact as possible. Then the discharge coefficient (α), describes the slope of this section. Depending on the actual recession curve, it may be necessary to differentiate certain parts of the recession if the discharge is originated by more than one linear store and thus just one trendline does not fit the whole system.

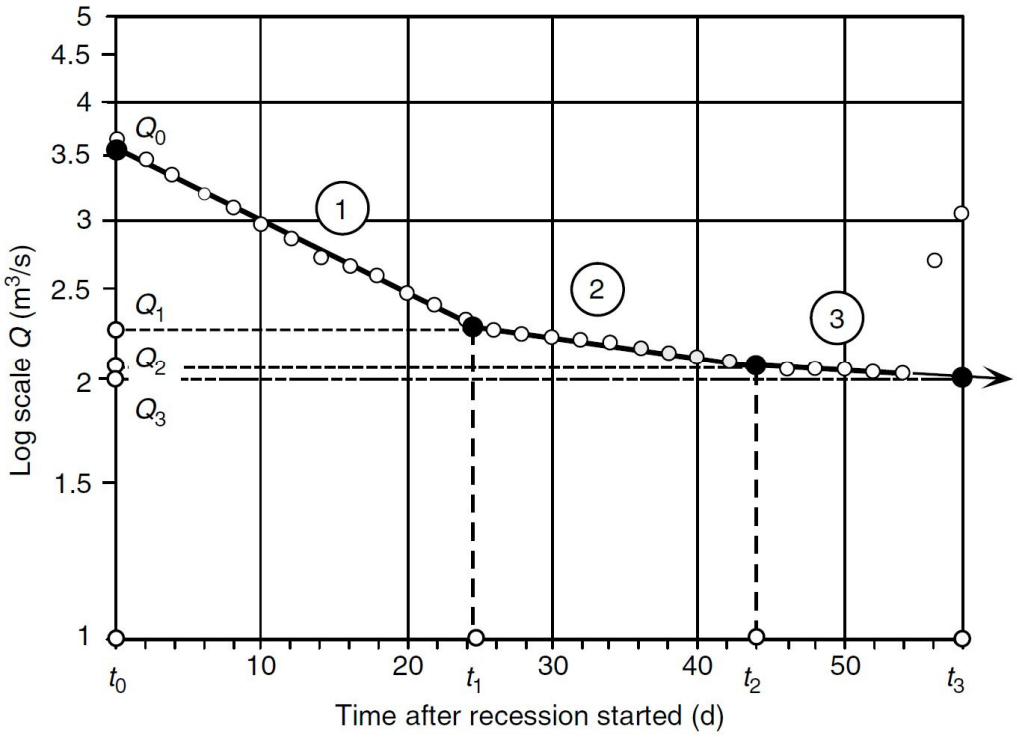

Figure 12: Semilogarithmic time - discharge diagram of an ideal recession period with three distinguishable discharge regimes (Kresic, 2007).

Equation 3: Maillet (1905) equation to describe discharge behavior.

$Q(t) = Q_0 \times e^{-\alpha t}$	Q(t): discharge [L^3/T] Q_0: discharge at time t=0 [L^3/T] α: discharge coefficient [1/T] t: time [T]

As described by Winkler et al. (2016) for the case of a relict rock glacier in the Seckauer Tauern Range (Austria), the linear storage model does not fit the entire aquifer range. It is shown, that the relict rock glaciers discharge behavior can be reasonably described by cutting the recession curve into at least three segments, i.e. exponential equations, which are each suitable to describe by an individual aquifer component.

Based on the known discharge at time t and the recession coefficient it is possible to calculate the volume of free water that is stored in the aquifer system at any time. The correlation between α and the still restrained water volume is shown in Equation 4. As described in e.g. Kresic (2007), thereby the volume of water at time t=0, i.e. start of the recession, furthermore the overall drained water volume of the recession period can be calculated.

Equation 4: Relationship between discharge coefficient and free gravitational water in the aquifer system.

$\alpha = \frac{Q_t}{V_t}$	Q_t: discharge rate at time t [L^3/T] V_t: Volume of water, stored in the aquifer [L^3] α: discharge coefficient [1/T]

Given a system with three distinguishable discharge coefficients, as shown in Figure 13, the total volume of water stored in the aquifer V_0, at the beginning of the recession, can be calculated as the

sum of the three individual volumes. Finally the total volume of water drained during the recession ΔV can be computed as shown in Equation 5, hence being the difference between V_0 and the remaining water volume at the end of the recession period V_x.

Equation 5: Calculation of the total drained water during the regarded recession period.

$V_0 = V_1 + V_2 + V_3$ $V_{out} = V_0 - V_{rem}$ $with: V_x = \frac{Q_x}{\alpha_3}$	V_0: Volume of water stored in the aquifer [L^3] $V_{1,2,3}$: Volumes of water assigned to the segments 1,2 and 3 [L^3] V_{rem}: volume of water remaining in the aquifer at the end of the recession period [L^3] Q_x: discharge at the end of the third microregime [L^3/T] V_{out}: Volume of water drained during the recession period[L^3] α_3: discharge coefficient of third microregime [1/T]

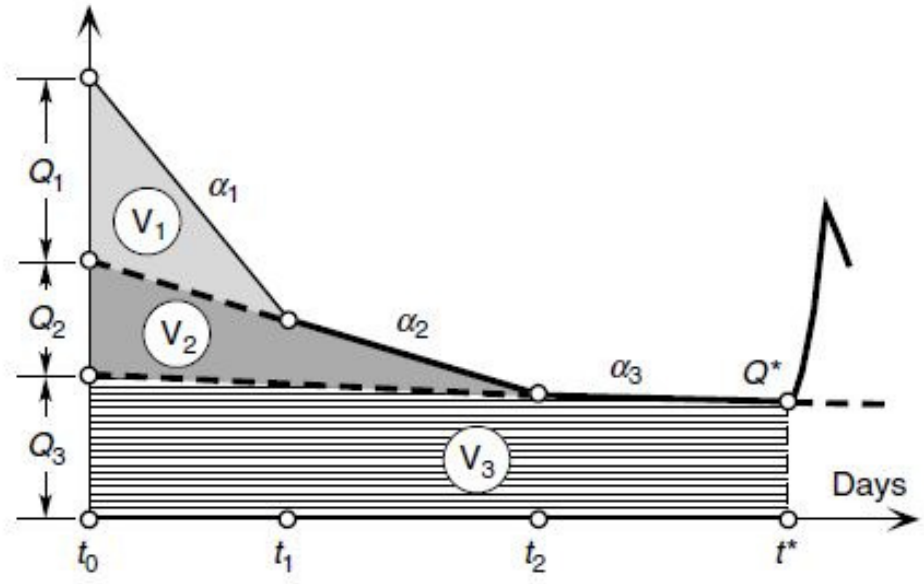

Figure 13: Time-discharge diagram showing a recession system divided into three segments with individual discharge coefficients. (Kresic, 2007)

3.3 Artificial Tracers:

Beside the natural tracers such as water temperature, electric conductivity and stable isotopes, the use of artificial tracers is well established in hydrogeology for the investigation of groundwater flow paths, flow velocities, retention time and others. As described by Ralf Benischke in "Methods in Karst Hydrogeology" (Goldscheider, et al., 2007), "artificial tracers are those injected or included by the investigator, for example fluorescent dyes, soluble salts or even flood impulses".

During the field work on the 31st July 2017 a tracer test was performed. In this case 202.49g of the fluorescence dye Uranine as a powder was dissolved in 2 l of water beforehand in the laboratory and transported in a light impermeable container, to avoid mixing problems or a loss of tracer on location and ensure a punctual tracer input. Uranine is very soluble in water and has a very low detection limit

of 10^{-3} µg/l in clean water (Goldscheider, et al., 2007). Negative aspects of uranine are that it decays when hit by sunlight or in contact with strong oxidants, i.e. acid environments. The tracer was injected on the 31.07.2017 at 17:08 o'clock. The injection point was the very last visible occurrence of a small runlet that infiltrates into the rock glaciers root zone (Figure 14). The detection is done with a field fluorimeter GGUN-FL30 (produced by Albilla Co., Neuchâtel, Switzerland) that was installed and started prior to the tracer input to create a reference null record. Furthermore, a water sample of the creek was taken for the calibration in the laboratory at University of Graz. The fluorometer was set up at the gauging station, this means that the cumulative runoff of the three main rock glacier springs is surveilled and no distinction about the exact flow path can be made. The fluorometer measured with a 2-minute interval until 02.08.2017 at 12:00 o'clock.

*Figure 14: Left: Tracer injection on the 31.07.2017 at 17:08 o*clock. Right: linear distance between the injection- and detection point.*

A second tracer test with uranine that was done on the 15th July 2015 in the course of the research for the previous masters thesis by Rieder (2017) is newly evaluated in this work.

Based on the Darcy`s law the hydraulic conductivity K can be estimated to further characterize the aquifer (Equation 6).

Equation 6: Calculation of the hydraulic conductivity derived from the Darcy Equation.

$K = \frac{v_f}{i}$ $v_f = v_a \times n_{eff}$	v_f: specific discharge [m/s] K: hydraulic conductivity [m/s] i: hydraulic potential h/l [/] v_a: apparent speed [m/s] n_{eff}: effective porosity [%]

3.4 Natural tracers

The common criteria for all natural tracers such as stable isotopes, organic solvents, chemical compounds, radiogenic isotopes, temperature and electric conductivity is their occurrence without any interference by an investigator (Goldscheider, et al., 2007). In the history of research at ÖGS rock glacier natural tracers always played a vital role, electric conductivity and water temperature was surveilled by Berger et al. (2004), the composition of stable isotopes are researched by Krainer et al. (2007) and finally Rieder (2017) combined the electric conductivity and water temperature to research the amount of event water in the total runoff.

3.4.1 Electric conductivity

The EC [µS/cm] of water is derived from its inverse, the resistance [Ω]. The EC is linked to the total dissolved solids TDS in the water by rule of thumb the larger the amount of TDS in the water, the higher the EC. Following Hölting et al. (2013) pure rainwater has an EC of 5 to 30 µS/cm, groundwater is in the range of 30 to 2000 µS/cm and from 1500 µS/cm upwards the term mineral water is used. The rock glacier environments are characterized by fast flow velocities, thus, the rock water interaction is limited and thereby the EC is referred to as a conservative tracer following Winkler et al. (2016).

The electronic conductivity record can be used to decipher the time lag between a recharge pulse and its signal at the measuring gauge. The concept relies on the assumption that the water creating the recharge pulse has a significantly different tracer signature (EC) which results in a deviation of the pre-recharge status. In this case the recharge pulse is created by either melting water or rainfall leading to a lower EC. The time lag is the period between the maximum infiltration (hydraulic pulse) and the associated deviation of the electronic conductivity. Maximum recharge is represented by the inflexion point of the rising discharge limb following Kovács et al. (2005). While the hydraulic pulse is quickly transmitted by the increase of the hydraulic gradient, the deviation of the tracer (EC) is measured when the event water arrives at the measuring gauge (e.g. Birk, et al., 2004). Maximum deviation of the tracer record, regarding the pre-recharge status, marks the breakthrough point of the newly recharged water (Winkler, et al., 2016).

3.4.2 Stable isotopes

Isotopes of the same element share the same atomic number, i.e. the number of protons, but differentiate in their mass number, i.e. combined number of protons and neutrons. They are called stable isotopes when the isotope itself is not radioactive. Thus, from the amount of neutrons, which is variable, follows a variation of the atomic weight. Using a mass spectrometer, the weight difference can be used to decipher the isotopic composition of a sample (Mortimer, et al., 2010). Each water molecule consists of two hydrogen atoms and one oxygen atom, both elements can occur in form of different isotopes with variable commonness. For the hydrogen this is mainly the ^{1}H (protium) and ^{2}H (deuterium), the oxygens three main isotopes are ^{16}O, ^{17}O and ^{18}O. Based on weight differences of the isotopes a kinetic fractionation occurs during fast and/or incomplete chemical reactions. This leads to a depletion and enrichment of certain isotopes in the educts and products of these reactions.

The sample analysis was done in the laboratory of JR-AquaConsol in Graz. Since the absolute amounts of isotopes is hard to determine and therefore imprecise, the convention is to state frequentness ratios in comparison to a standard (Equation 7). These ratios are called delta notation, usually the value is given in per mill deviation from the standard. As a standard for hydrogen and oxygen in water the “Vienna mean standard ocean water (VSMOW)” provided by the “International Atomic Energy Agency (IAEA)” is used.

The influence of certain environmental conditions on the isotopic composition of water is a well-researched topic (e.g.: Clark, et al. 1997; Mook, 2001; Leibundgut, et al.,2009; Clark, 2015), a basic summary of the effects is displayed in Figure 15. All the unattached water in the area was meteoric water at some time. In the research area several of these fractionation effects come into play. As the research area lies in the central alps it contains significant altitude differences, a strong seasonality and the meteorological influence of both the Atlantic Ocean and Mediterranean Sea. Additionally, there is ice in form of the Hinterer Ölgrubenferner as well as the rock glacier ice core that can most likely be distinguished in their isotopic composition from the present meteoric waters due to different climatic settings during the former precipitation of these water molecules.

With the help of oxygen and hydrogen isotopes the origin of spring water shall be deduced.

Equation 7: δ-notation of isotope samples.

$\delta = \left(\frac{R_{sample}}{R_{standard}} - 1\right) \times 1000$	R: Isotope ratio, usually rare/common

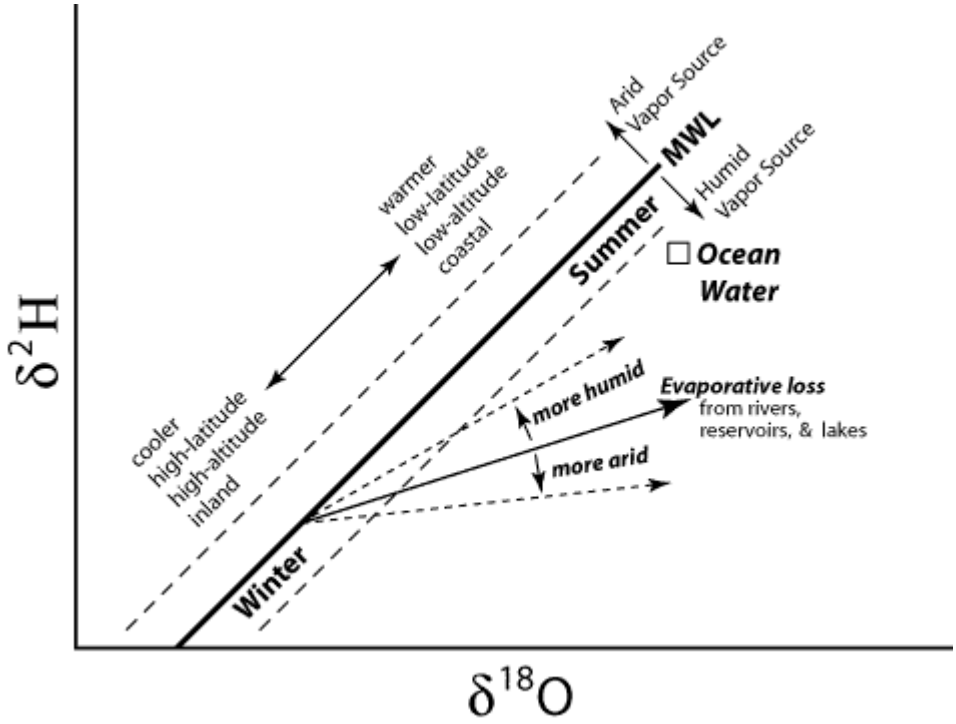

Figure 15: Influence of the environmental conditions on the isotope composition of water (Clark, et al., 1997).

3.4.3 Flow component separation

Since the electronic conductivity is permanently recorded at the water gauge its variations can be linked to other records of temperature, discharge and isotopic composition. This allows to distinguish certain discharge regimes and their percentage of the overall runoff. Furthermore, the duration of the influence of a precipitation event can be computed with this data. Wels et al. (1991) provide a formula that allows the separation of runoff into two sources with different tracer concentration, originally isotopes and weathering products were used. The equation was refined by Winkler et al. (2016) by replacing the tracer concentration with the conservative tracer "electric conductivity" (Equation 8). Both approaches assume that the change in the values is solely induced by the mixing of the two components, i.e. pre-event water and event water.

Equation 8: Calculation of the amount of event water (Winkler, et al., 2016).

$Q_n \approx Q_s - \frac{EC_S - EC_P}{EC_{old} - EC_P} \times Q_S$	Q_N: event water [l/s] Q_S: total discharge [l/s] EC_S: EC of spring water [µS/cm] EC_P: EC of precipitation water [µS/cm] EC_{old}: EC of pre-event water [µS/cm]

The runoff as shown by a hydrograph is the result of discharge typically based on different flow components. Depending on the contemplated hydro(geo)logic system at least three components can be distinguished (Hölting, et al., 2013). The baseflow, which can be observed after an extended period of time without any significant recharge and is usually considered as groundwater fed. The interflow, as the part that is fed by near surface layers, where the water moves almost horizontally, parallel to the surface and contributes to the discharge shortly after the precipitation. Finally the direct flow, the sum of the surface discharge and the interflow. This classification is usually applied on stream-flow, the application on the discharge of alpine-, especially rock glacier dominated systems may need some adaptations.

Highly variable systems with preferential flow paths, such as karst springs, which somehow show comparable discharge behavior to rock glacier systems (e.g.: Gödel, 1993; Winkler, et al. 2016; Pauritsch, et al., 2017) may require customized separation criteria and nomenclature. Furthermore, due to the alpine environment and its various forms of precipitation and water storage, the flow components can show all possible superposition effects so that discharge separation must be done in a customized manner depending on the local situation.

4 Results

The results are based on the data set displayed in chapter 2.4, established during the field trips in 2017 and further data of previous investigations (all data older than 31.07.2017) from the field site ÖGS.

4.1 Runoff Log / Hydrograph

The alpine area in which the field work takes place claims some tributes, data gaps and uncertainties are not entirely avoidable. For this reason, the data evaluation and utilization needs some adaptations and data processing that are worth being described in this chapter to be able to classify its quality.

4.1.1 Water level

The three main springs of the ÖGS rock glacier summon after a few dozen meters in one small stream. A gauging station equipped with two different data loggers was installed several years ago by the Prof. Karl Krainer and his team (University of Innsbruck). Despite some errors (?) and data gaps a reasonable water level data set for the years 2014 to 2017 is available. Due to the high alpine environment the data recording is challenging and thus some data processing is needed. Runoff data of two loggers had to be matched to create a single series with as little gaps as possible. After the correction of the data from each data logger concerning apparent measuring errors, the two loggers series show a good linear correlation, shown in Figure 16 and Table 1. While the two loggers show a clear shift in their values, the dynamics recorded are alike. It is assumed that each logger works correctly and the gaps, where only one of the two loggers worked, can be filled by the remaining running logger.

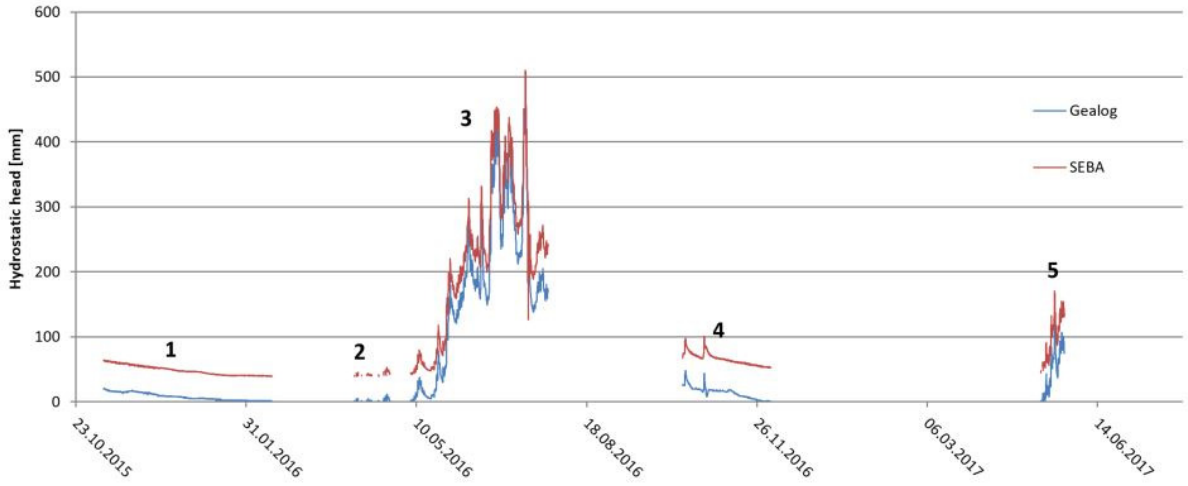

Figure 16: Data logger record of the two devices "SEBA" and "Gealog". Data is only plotted for periods where both loggers recorded simultaneously.

Table 1: Pearson correlation coefficients (PCC) as calculated for the two data loggers on data series as shown in Figure 16.

Period:	**1**	**2**	**3**	**4**	**5**	
Time span:	8.11.15 - 15.2.16	3.4.16 - 24.4.16	6.5.16 - 26.7.16	13.10.16 - 5.12.16	11.5.17 - 25.5.17	overall period
PCC:	0.982	0.872	0.994	0.903	0.994	0.996

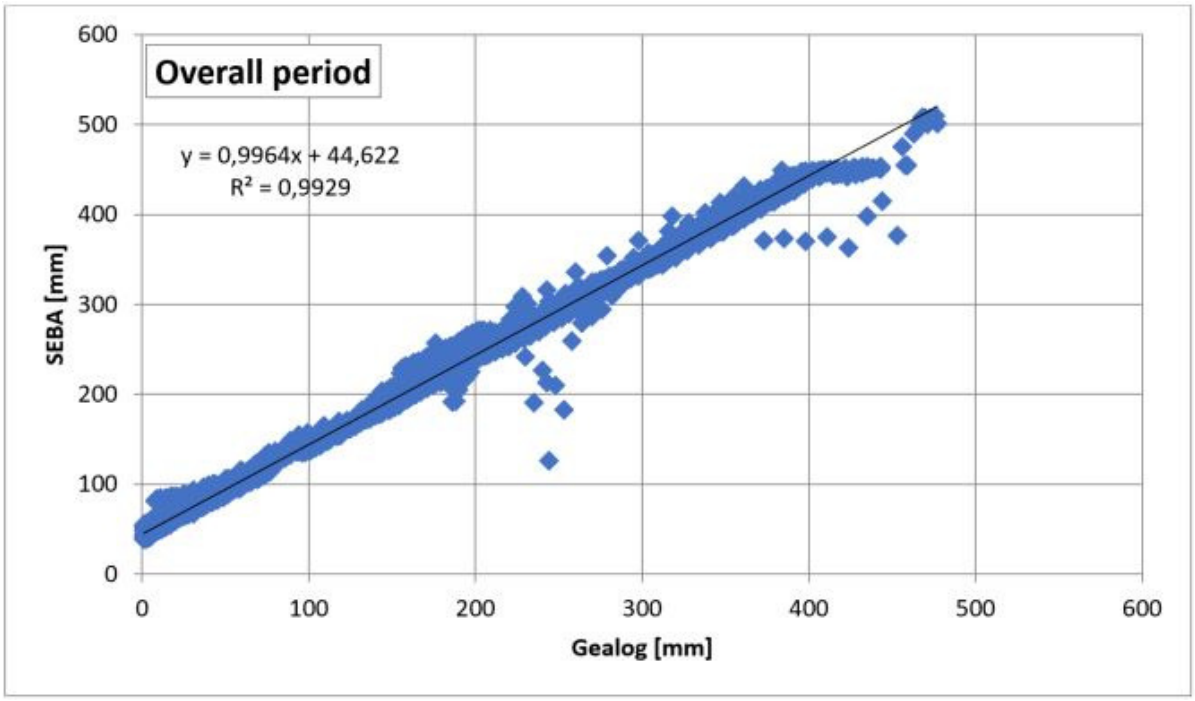

Figure 17: Correlation plot with entire corrected Gealog and SEBA logger data as shown in Figure, showing a linear correlation.

Due to these results the data from the Gealog probe is shifted to fit the SEBA probe. Since the Seba probe is apparently placed slightly lower, it didn't fall dry as fast as the higher placed Gealog probe and therefore has an extended record in low water periods. Caused by the situation of the gauging station, the shift between the two loggers isn't constant. Data is empirically adjusted for periods with constant deviation to get a continuous composite hydrograph as shown in Figure 18. The regarded record starts on the 01.06.2014 and end in the summer of 2017 on the 12.06.2017 due to technical problems with the data loggers. Two gaps, one in the late spring of 2015 and one in the late summer to autumn 2016, could not be filled despite the redundancy again due to technical problems with the data loggers. Nevertheless one hydrological year's discharge at the ÖGS rock glacier is recorded and conniving the two gaps a comparable discharge behavior can be assumed for the three year long record.

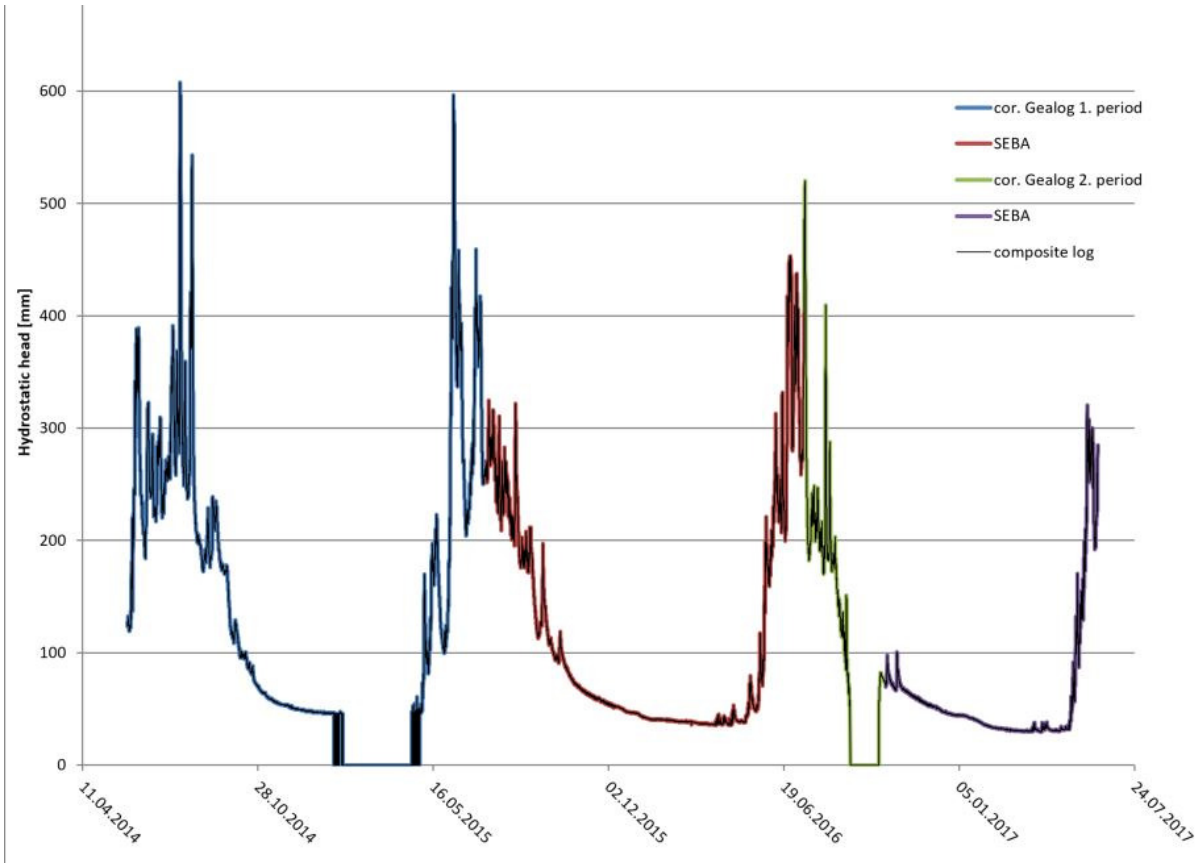

Figure 18: Final "composite hydrograph" after correction of the periods shifts and data processing.

4.1.2 Rating curve

During the field days from the 31.07.2017 to 02.08.2017 several discharge measurements with the salt tracer method were performed at different daytimes, in order to cover the broadest possible discharge spectrum. Since hydrological investigations at ÖGS rock glacier date back well over 10 years, many more runoff measurements were done and the results are kindly provided by Karl Krainer.

During the measurements in summer 2017 some difficulties with the mixing of the salt tracer became apparent. As described in the methods section, it is necessary to achieve a complete homogeneous distribution of tracer in the creeks water for this method. Two probes were placed in promising spots slightly off center in small ponds at the left and right side of the creek. The deviation of the results between the two probes is up to about 20% of the total value which indicates an insufficient mixing of the tracer with the creeks water.

Ultimately the measurements from summer 2017 cannot be used for the rating curve generation. Because of the malfunction of the data loggers at mid-June 2017, no data to correlate the discharge measurements is available, too. The rating curve (Figure 19) is based on discharge measurements provided by Karl Krainer, from the years 2014 and 2015. Again, the discharge measurement was performed with two probes and shows a similar lack of homogenization that finally leads to an uncertainty spread especially for higher values.

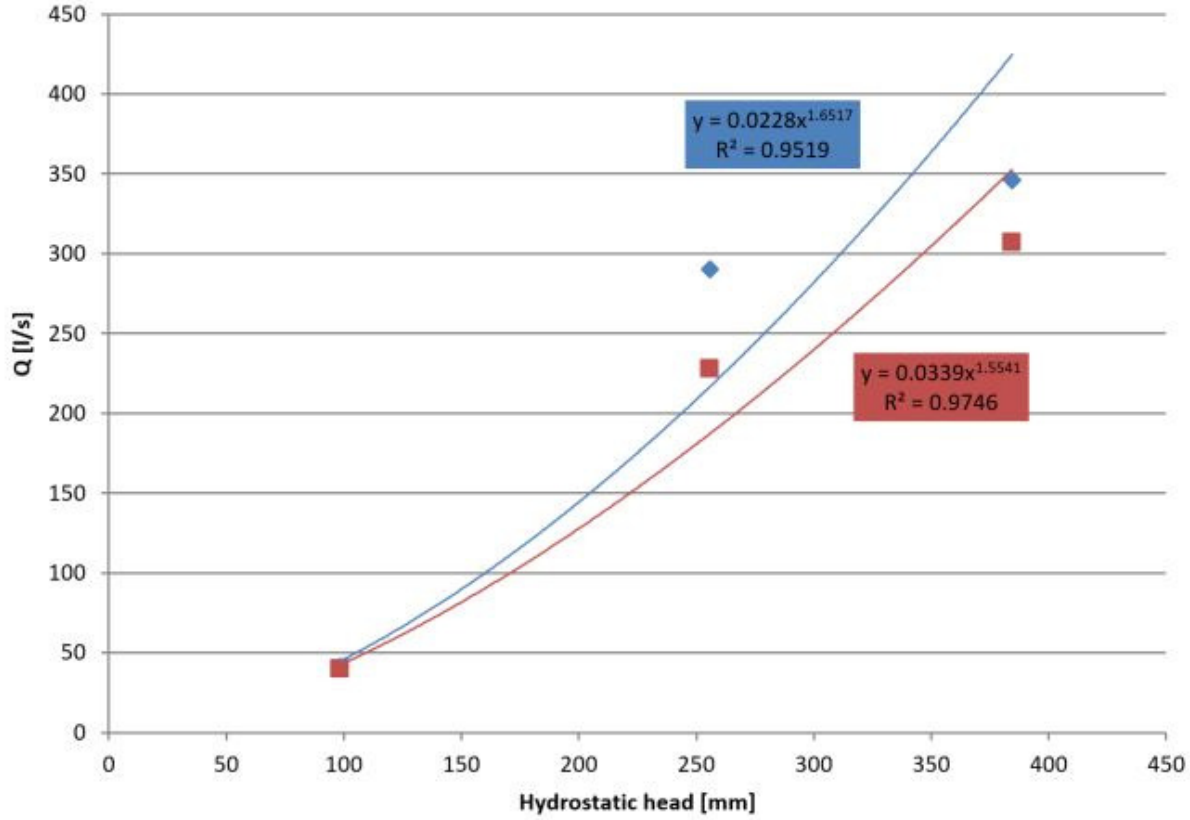

Figure 19: rating curves generated in Microsoft Excel for ÖGS rock glaciers main draining creek. Note the deviations in the discharge measurement results in two slightly deviating curves. Blue: higher discharge measurement. Red: lower discharge measurement.

Since the rock glaciers creek is of very irregular shape (?) and reference measurements with the salt tracer method are limited to fair weather periods in summer, especially the lower and upper extremes of the discharge values are considered somewhat uncertain, but the dynamic is most likely correct. With this knowledge the flatter rating curve (red) defined by the following equation:

$$y = 0.0339 * x^{1.5541}$$

is used for the further calculations.

4.2 Hydrograph analysis

Combining the rating curve $y=0.0339x^{1.5541}$ from the previous steps with the hourly measurements from the water gauge (compare Figure 18) a hydrograph showing the runoff vs. time behavior can be set up (Figure 20). The reviewed period is identical with the length of the "composite hydrograph" assembled and displayed in Chapter 4.1, from 01.06.2014 until 12.06.2017. At first glance an annual runoff rhythm is unmissable, the maxima are all reached in June and July each year, while the minima are recorded in late March and April. Each year, after the minimum is reached, the runoff increases quickly from just about ten l/s to a few hundred l/s in only a few weeks. During the summer until the end of autumn, the behavior is very variable showing many local minima and maxima, but the amplitude of the variations roughly decreases towards the end of the year. Afterwards, beginning approximately in November, a nearly undisturbed recession period can be observed in all three

reviewed years. Since the measurements for the rating curve do not include states with very high nor very low runoff, the extreme values have some uncertainty.

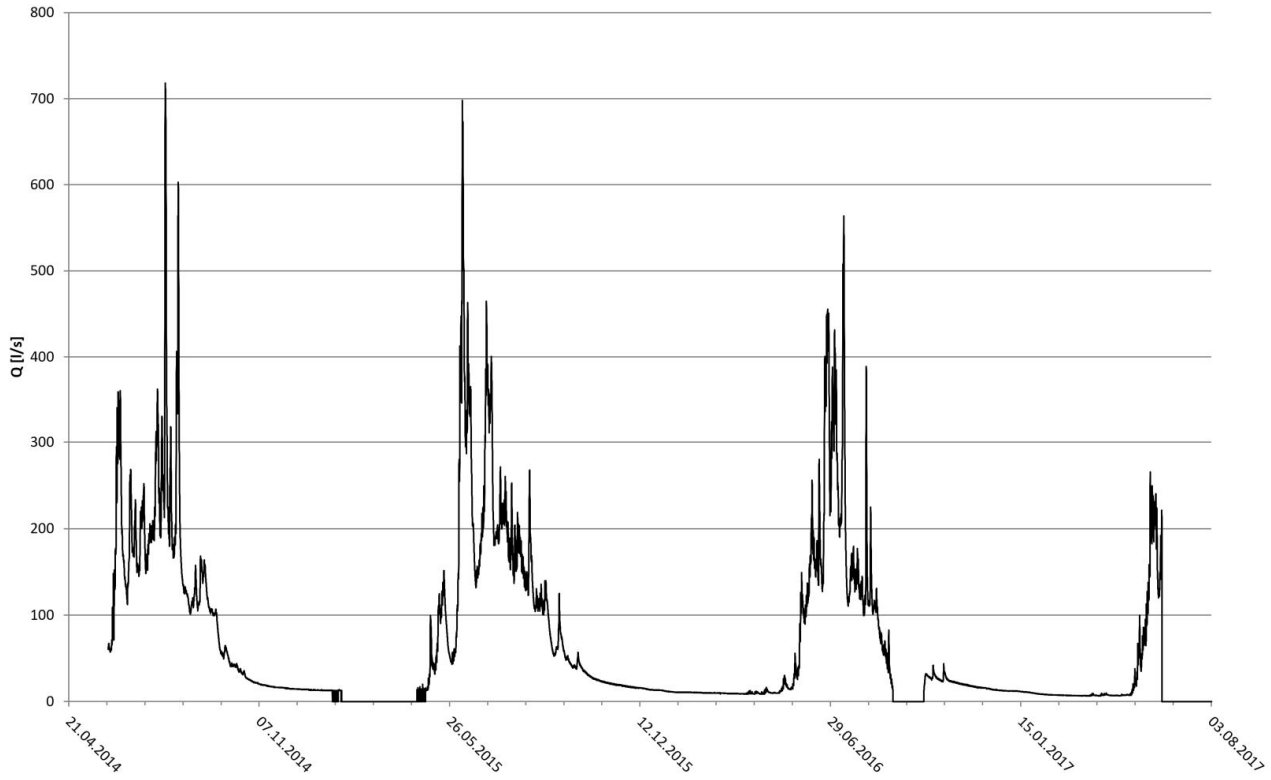

Figure 20: Hydrograph at the gauging station near the front of ÖGS rock glacier. Computed with the rating curve $y=0.0339x^{1.5541}$ *and the compiled hydrostatic pressure record (Figure 18). Null values are data gaps and can be ignored.*

The displayed data is coherent with previous work from Rieder (2017) and Berger et al. (2004) done on ÖGS rock glacier.

Figure 21 exhibits data from 05.06.2015 until 31.03.2016 showing the total possible range of the hydrological year 2015 as an example. Furthermore, the situation in august 2015 is highlighted to illustrate the typical daily runoff behavior. Several different types of amplitudes can be distinguished. During the summer, a daily small-scale variability in the range of about 25 l/s is visible, its maximum is usually reached in the early morning while the minimum tends to occur in the late afternoon or early night. Exceeding the daily variations, the record shows erratic ascends followed by sharp descents, these deflections usually last from hours up to several days and cause the characteristic spike pattern of the hydrograph record. The variation in amplitude and duration indicate roots in a bigger scale and more unsteady phenomenon as the daily variations. Finally a long-term pattern with a steep escalation from May to mid-July and subsequent a near exponentially formed descent can be detected at a closer look.

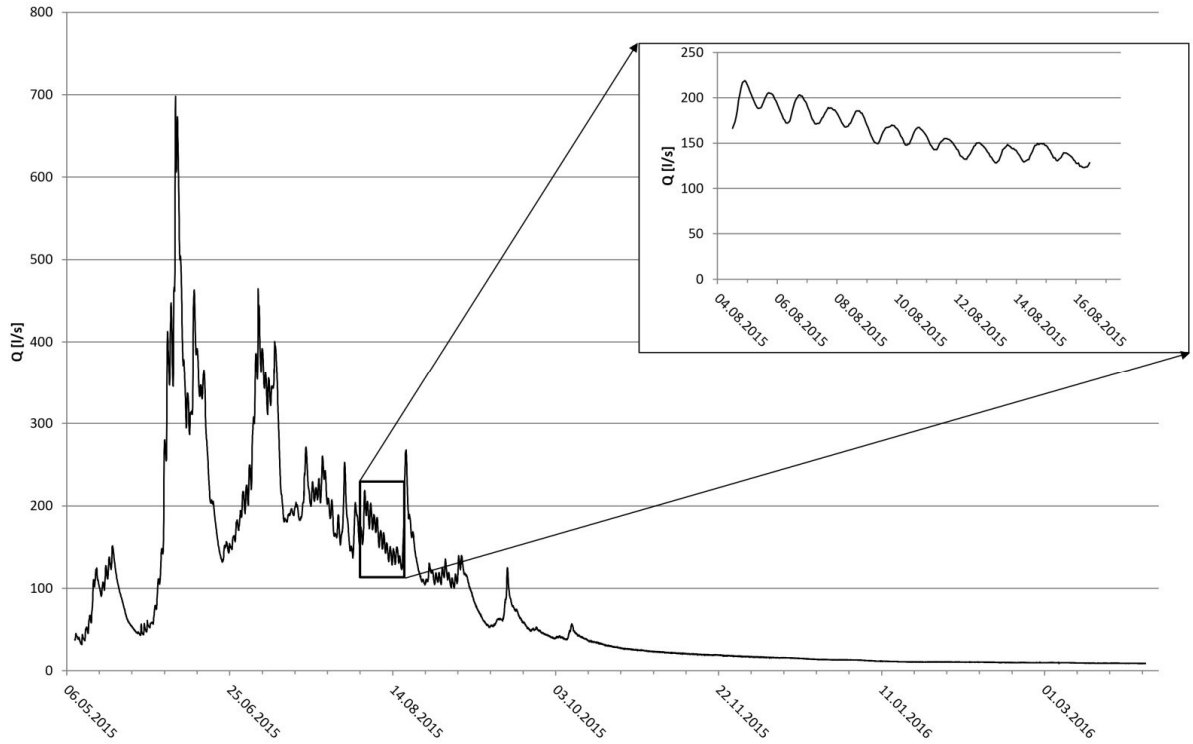

Figure 21: Hydrograph for the period of 05.06.2015 until 31.03.2016, with detail window showing the daily amplitude in mid-summer.

Discharge quotient:

As described in section 3.1 a discharge quotient can be calculated for each hydrological year. In this case a hydrological year is the period between two measured minimum baseflows. The relation between the highest Q_{max} and lowest Q_{min} measured runoff indicates the retention capabilities of the aquifer. Note that the runoff data is the compound of three main springs at the front of the ÖGS rock glacier but the contribution of a significant surface runoff after heavy rainfall cannot be ruled out. The results can be seen in Table 2, due to the data gap in early 2015 the real Q_{min} is most likely not recorded for this year, leading to a slightly higher discharge quotient. Following Hölting et al. (2013) the displayed numbers are values for a highly variable aquifer system such as karst.

Table 2: Calculated discharge quotients for the hydrological years 14-17.

Hydrological year:	**Q_{min} [l/s]**	**Q_{max} [l/s]**	**Q_{min}/Q_{max} [/]**
2014/2015	13	718	0.018
2015/2016	9	698	0.013
2016/2017	7	564	0.012

Master recession curve analysis:

For the compilation of the Master recession curve with Posavec et al. (2017), the discharge measurements are averaged from the hourly record to a daily average. This is done to smoothen the graph and rule out some of the short-term variations that would interfere the prioritized long-time analysis. Plotting the data into a semilogarithmic diagram (Figure 22) already shows the recurring baseflow periods during the winter and early spring each year.

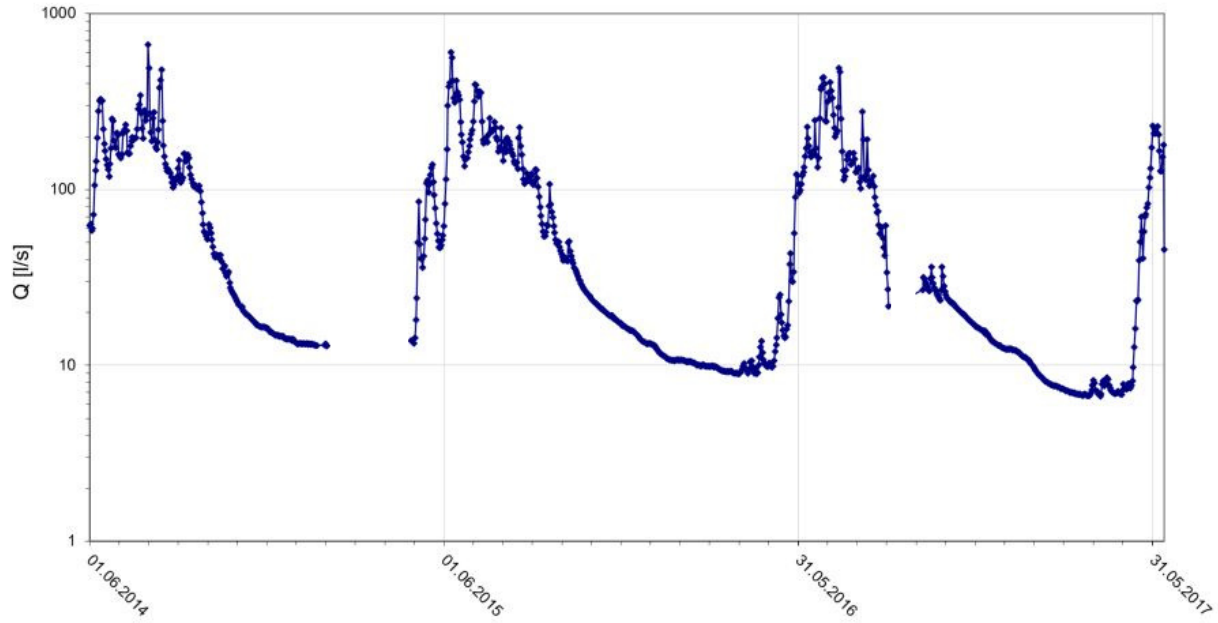

Figure 22: Semilog time-discharge plot showing the daily mean runoff from 01.06.2014 to 12.06.2017 at ÖGS rock glacier.

The time-discharge record with the daily mean runoff values, displayed in Figure 22, is cut into the three recorded hydrological cycles. For these three periods, as well as on the total record, a MRC is compiled and analyzed. The segmentation is done at the last measured minimum of each period, before a significant and persistent rise of runoff is recorded and a new period starts. The exact dates are shown in Table 3, again the record gaps in 2015 and 2016 complicate the direct comparison of the three periods.

Table 3: Recession coefficients for each period calculated following Maillet (1905).

Period:	**From:**	**To:**	**α_1:**	**α_2:**	**α_3:**
2014/2017	01.06.2014	12.06.2017	0.163	0.022	0.005
2014/2015	01.06.2014	31.01.2015	0.467	0.078	0.005
2015/2016	01.05.2015	31.03.2016	0.149	0.028	0.003
2016/2017	01.04.2016	27.03.2017	0.218	0.020	0.005

An example of a MRC created with the Microsoft Excel VBA script by Posavec et al. (2017) is displayed in Figure 23, the script divides the record into periods of constant recession and queues them depending on their start value, which is the highest value of the record snippet. Plotted in the semilogarithmic diagram, periods which form a straight line follow a behavior that can be described with Maillets (1905) linear runoff model as described in Equation 3 (Kresic, 2007). Areas of similar runoff behavior are manually fitted with a line, the lines gradient is the so-called recession coefficient "α". Three different microregimes can be distinguished. They are each represented by their own line (black, green, orange) and corresponding discharge coefficient.

Displayed in Table 3, the discharge coefficients of the three inspected periods and the overall record show a consistent pattern. The three microregimes coefficients are separated by a factor of 5 to 11 from their neighboring regime and show little deviation through the years. The period 2014/2015 is a bit conspicuous in the first two microregimes, the reason may base on the short recession record of this period. Despite that, especially the baseflow represented by α_3 replicates itself each year indicating a stable and independent basic system.

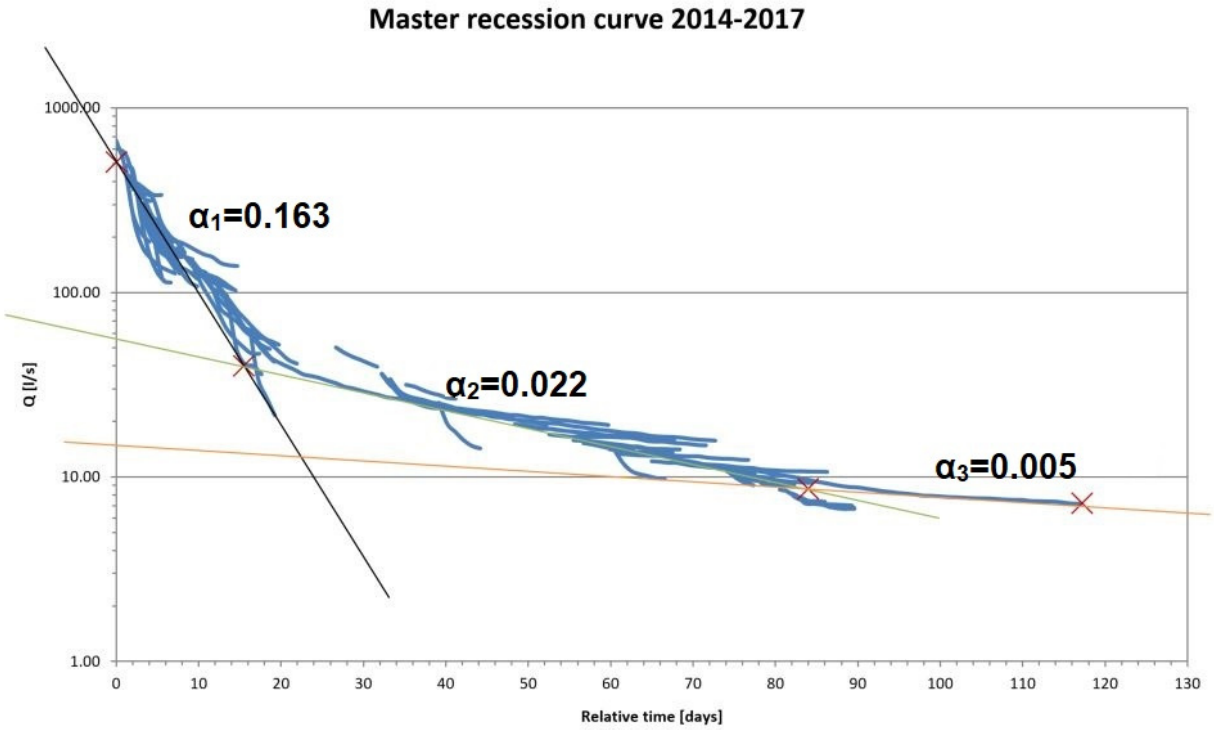

Figure 23: Master recession curve for the total record from 01.06.2014 to 12.06.2017. Including the manually fitted lines, describing the discharge behavior of their respective microregime.

Storage volume:

Given the calculated discharge coefficients, the initial volume V_0 of water prior to the recession, the amount of water V_{out} that is drained during one period and the remaining volume V_{rem} of water stored in the aquifer at the end of the recession can be calculated as described in section 3.1. This is done by taking the discharge coefficients from Table 3 and applying Equation 5, leading to a remaining volume of water between 0.121 x10^6 m^3 and 0.302 x10^6 m^3. Looking at the total water volume at the start of the recession the highest value is 0.965 x10^6 m^3 in the period 2015/2016, considering an average effective porosity of 0.2 for the aquifer and the rock glacier having a surface of 23.8 ha a theoretical thickness of the aquifer of about 20 m is needed to store the water. The calculated volumina for the other two periods would result in a needed aquifer thickness of 15 m (2014/2015) and 11 m (2016/2017).

Table 4: V_0: Initial water volume -; V_{rem}: remaining water volume -; V_{out}: total discharge during the recession; t.a.h.: theoretical aquifer height with assumed porosity of 0.2 and a surface area of the ÖGS RG of 238029.7 m^2.

Period:	V_0 [x10^6 m^3]	V_{rem} [x10^6 m^3]	V_{out} [x10^6 m^3]	t.a.h. [m]
2014/2015	0.704	0.259	0.445	20
2015/2016	0.965	0.302	0.663	15
2016/2017	0.538	0.121	0.417	11

Regarding the calculated volumina in Table 4, a difference between the period 15/16 and 16/17 concerning the remaining volume of more than 100 % is striking. Since rock glaciers are said to have good retention capabilities these differences in the remaining water volumes need to be accounted for.

4.3 Artificial tracer test

The tracer tests data as performed in the summer of 2017 from the 31st of July to the 2nd of August is displayed in Figure 24. The recovery rate is shown with error bars of 10% to incorporate uncertainties in the actual discharge rate during the time where the test was performed. The tracer was injected on the 31.07.2018 at 17:08 o'clock. First detection and thereby proof of connectivity is 2 h and 34 min. later, given the linear distance of 850 m this leads to a maximum effective velocity v_{max} of 0.092 m/s. The peak concentration of 45.6 mg/m^3 is reached after 5 h and 20 min hence the dominant flow velocity is v_{peak}=0.044 m/s. 50 % tracer recovery is recorded after 6 h and 18 min, which results in a mean velocity v_{mean} of 0.037 m/s. Following Benischke et al., the effective mean travel time lies in between v_{peak} and v_{mean} in most cases (Goldscheider, et al., 2007). Since the difference is insignificant an effective flow velocity $v_{eff.}$ of 0.04 m/s is assumed.

The tracer recovery rate is in the range of 85-100 %, this indicates that the vast majority of the water that infiltrates the rock glacier at the injection point is not stored longer than a few days. The falling limb of the concentration is without any interfering peaks and additionally the concentration record is characterized by a sharp ascent and descent, which means that the tracer cloud most likely took one preferential flowpath instead of being split up and deferred.

Table 5: Comparison between the main results of the tracer test performed in 2017 and the newly evaluated one from 2015 by Rieder (2017).

Date	Injection time	First detection	Peak concentration	50% recovery	Linear distance	v_{max} [m/s]	v_{peak} [m/s]	v_{mean} [m/s]	$v_{eff.}$ [m/s]	Recovery rate
15.07.2015	11:20	2h 40 min	4h 28 min	8h 7 min	1060 m	0.110	0.066	0.036	unknown	55%
31.07.2017	17:08	2h 34 min	5h 20 min	6h 18 min	850 m	0.092	0.044	0.037	0.04	≥85%

The 2017s tracer tests maximum effective velocity can now be used to calculate the hydraulic conductivity K. Following Winkler et al. (2016) an effective porosity of 0.2 is assumed for the rock glacier and a hydraulic potential (h/l) lead to:

$$i = \frac{h}{l} = \frac{290\,m}{850\,m} = 0.34$$

$$v_f = v_a \times n_{eff} = 0.092\frac{m}{s} \times 0.2 = 0.018\frac{m}{s}$$

$$K = \frac{v_f}{i} = \frac{0.018\frac{m}{s}}{0.34} = 5.3 \times 10^{-2}\frac{m}{s}$$

The calculated hydraulic conductivity K=5.3 x 10^{-2} m/s is characteristic for a very well permeable aquifer (Hölting, et al., 2013).

The data of a second uranin tracer test that was conducted in 2015 by Rieder (2017), is newly evaluated during this masters thesis. The differences are mainly in the adjusted discharge curve which is shown in chapter 4.1. For the new tracer recovery calculation, the newly computed runoff data is used resulting in slightly different recovery values. Comparing the results of this tracer test with the newly evaluated data of the tracer test performed in 2015 by Rieder some similarities and differences can be seen (Table 5, Figure 24 and Figure 25). Both tests show a fast connection within a few hours that transported a majority of the detected tracer material and thereby approve the existence of a preferential flow path. The minor recovery rate of the 2015 tracer is possibly a sign for a retention of some of the water and might be released in non-detectable small rates. Since the amount of used

tracer was only 25 g compared to the 202.49 g in 2017, the signal is not as strong due to the higher dilution factor.

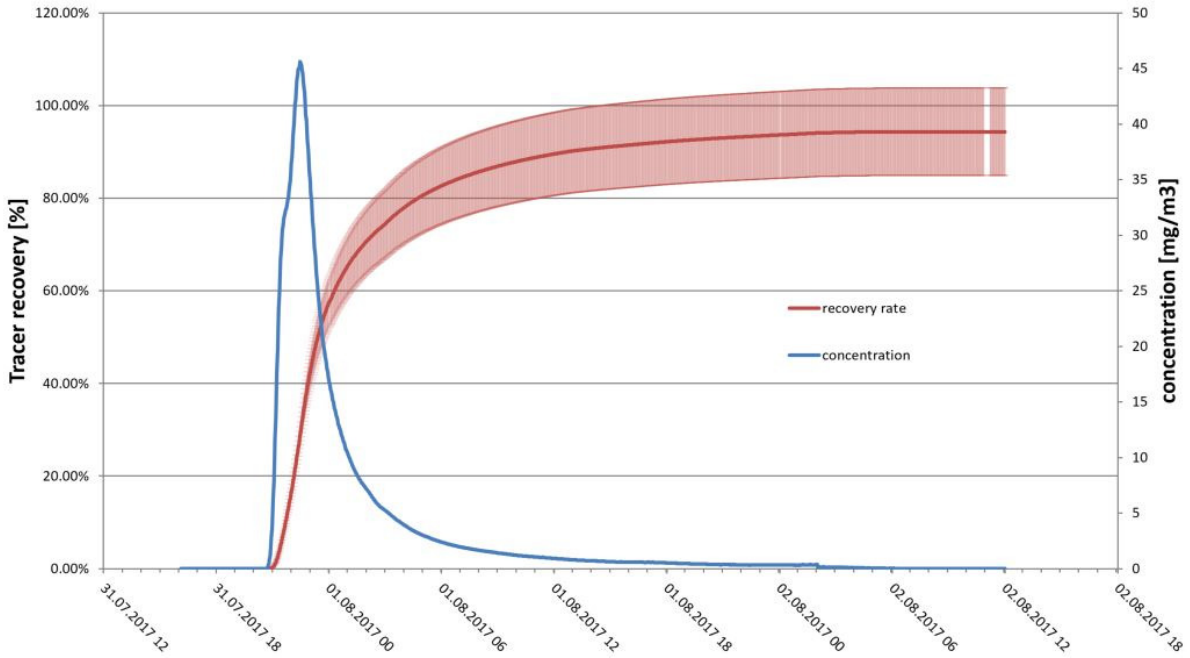

Figure 24: 2017s tracer test recovery and concentration. The error bar for the recovery rate show an assumed 10% error regarding uncertainties of the actual discharge.

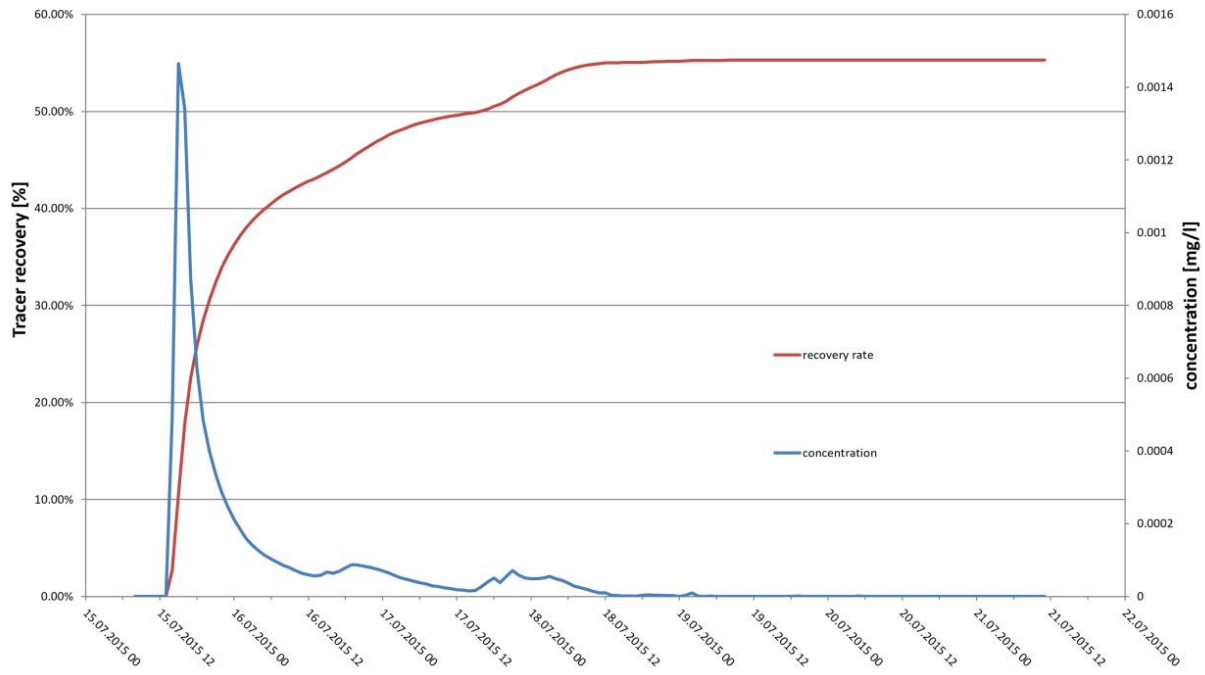

Figure 25: 2015s tracer test recovery and concentration diagram. Tracer data acquired by Rieder (2017).

4.4 Natural tracers

4.4.1 Electric conductivity

Manual measurements:

The electric conductivity of the water was standardly measured at the isotope sampling locations (Figure 7) when taking samples. The values are given in Table 6 and are displayed together with the isotopic data in Figure 30. Overall the measured values range from 1.2 µS/cm at HK01 (melted ice) to 505 µS/cm at HK05 but the spread at each single location is far less, although distinct. The lowest spreads are calculated for the springs (RA) with max/min being 2.2 and 2.3, while the highest spreads are found at HK02 and HK03 with 11.1 and 10.7. All the minimum and maximum values where measured the same days 01.08.17 (min.) and 15.09.17 (max.), that a connection causing this phenomenon on the rock glacier system can be assumed. Generally, the measurements in the catchment area (HK) show a rise in the EC inverse to the height of the location, i.e. from the Hinterer Ölgrubenferner to the infiltration area of the streamlet at the rock glaciers root zone. Comparing the EC of the infiltrating water (HK04 and HK05) with the spring water (RA), it can be stated that the EC of the infiltrating water is never quite reached by the spring water. This indicates a mixing with a water source with lower EC inside the ÖGS rock glacier. A connection of the weather data with the EC of the water is made and described together with the isotopic data in the following subchapter.

Values at RA03 are generally higher than RA01 and RA02. RA03 is located at a spring bellow the smaller southern tongue of ÖGS RG, the reason for the enhanced EC is unclear, it might be caused by lithological differences, preferential flow path of the infiltrating water towards RA01 and RA02 or variations in the storage capabilities.

*Table 6: Manually measured electric conductivities at the isotope sampling locations. The lowest and highest value of each location is written italic. The location HK01s values can be considered as pure ice samples. Values given in **µS/cm**.*

Location:	01.08.17 am	01.08.17 pm	02.08.17	10.08.17	15.09.17	max/min:
HK01	***1.2***	**/**	**1.4**	**1.6**	***4***	**3.3**
HK02	*27.5*	/	34	41	*304*	11.1
HK03	*27.6*	32.5	33.6	39.2	*296*	10.7
HK04	*118*	121	127.9	150.5	*414*	3.5
HK05	*117*	121	126.5	149.6	*505*	4.3
RA01	*90.7*	102	96.5	107.6	*200*	2.2
RA02	*97.8*	108	101.2	113.9	*229*	2.3
RA03	*136*	144	141	145.2	*296*	2.2

Continuous measurements:

While the infiltrating water/brook and the individual springs were only measured 5 times, the SEBA probe at the gauging station continuously recorded the EC in one-hour intervals. The graphs displayed in Figure 26 give insight into the relation of EC and current runoff. While the EC log is only measured by the SEBA data logger, the runoff is recorded by both Gealog and SEBA sensors, thus there are runoff measurements in times where the SEBA probe fell dry and no EC is recorded. In Figure 26 graph a) and c) the rapid decrease of the EC values towards the end is where the probe loses contact to the water.

Graph a), b), c) and d) of Figure 26 give a detailed view on the sections (marked in the upper overview graph) where both EC and runoff are recorded. The highest recorded EC value is 281 µS/cm on the

06.11.2015 while the lower end of the spectrum is somewhat beneath 80 µS/cm. As visible in the overview and graph a) and c), the EC rises with decreasing runoff values reaching the highest measured values in November of each year.

Graph a) and the section from 15.07. to approx. 15.08.2015 reveals a slightly rising EC accompanied by the overall decreasing trend of the discharge. The EC inversely follows the discharge curve and daily variations but shows only damped amplitudes in comparison to value swings negatively correlating with runoff peaks later in the year. After an interruption in the continuous development due to increased runoff as a result of rainfall and a few more days of daily variations, the record in both runoff and EC changes abruptly at the beginning of September 2015. Daily variations are damped to an indistinguishable level and the runoff record shows the development towards the undisturbed baseflow. The transition into the recorded baseflow is interrupted by three distinct peaks and their matching minima in the EC record.

Graph b) starts on the 20.05.2016 and ends on the 26.07.2016, the time corresponds with the snow melting season. Again EC shows inverse behavior to the runoff with nearly simultaneously reaction. Discharge rises and after one week daily variations can be seen in the EC and discharge record. The high EC values (max 221 µS/cm) in the first week are probably caused by a significant part of pushed out groundwater that reacts on the infiltration impulse of the melting water. The daily discharge variations are not pronounced enough to be seen in runoff nor EC data until early June. Runoff peaks at the end of June and in July do only show damped signals in the EC record as previously described. As opposed to a heightened runoff, the contrary falling runoff induces significant signals in the EC log, this can be observed around the 20.06. or 17.07.2016.

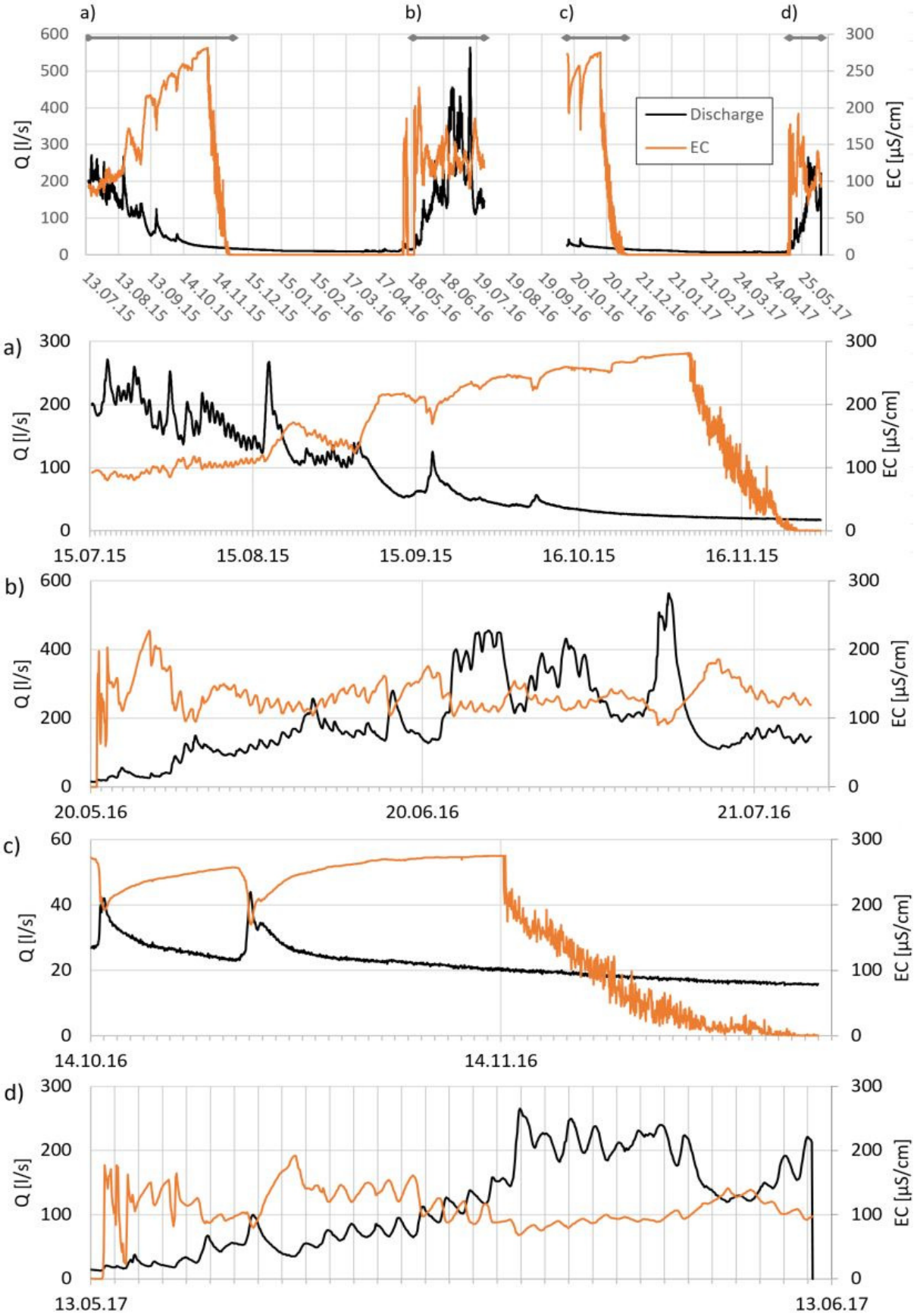

Figure 26: Detailed view on the discharge behavior and corresponding electronic conductivity measured at the water gauge from 15.07.2015 to 12.06.2017. Diagram a), b), c) and d) give further insight into the system from a wider several month long overview down to the daily cycles. The discharge plot is the compound of the Gealog and SEBA data logger as described in chapter 4.1.

Graph c) displays the data from 14.10.2016 to 07.12.2016 and thereby the transition from the rainfall and melting water affected system into the baseflow-period with no recharge. Note the smaller Q-axis, little changes in runoff are more pronounced! Neither the EC nor the runoff log show daily variations, an indication that the mean air temperature of the catchment area has dropped below the melting point (compare to graph a)). Two rain events cause sharp peaks that are accompanied by the EC-log with the respective minima. A maximum EC of around 280 µS/cm is measured before the logger fell dry in mid-November.

For Figure 26 d) basically the same explanations as for the first part of graph a) apply. The section begins on the 13.05.2017 and ends on the 12.06.2017 showing the first full month of the melting season. A several days lasting period (30.05. to 08.06.2017) of increased discharge is accompanied by damped daily variations in the EC log. Figure 27 displays a week-long subsection from 20.05. to 27.05.2017, showing that the daily variations in discharge and EC are simultaneous in undisturbed dry periods. Then the amplitude of the daily EC variation is about 25 to 40 µS/cm.

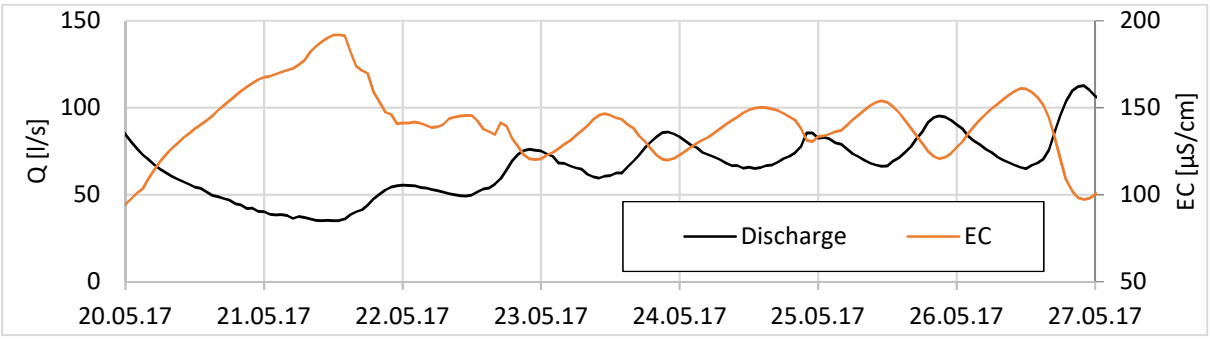

Figure 27: Detailed view of a subsection of Figure 26 d) showing the daily variations in runoff and EC.

Regarding the recorded EC vs. Q, as plotted in Figure 26, a time lag analysis was conducted for 45 recharge events between 17.07.2015 and 11.06.2017. The average time lag between the strongest hydraulic pulse and the breakthrough of the EC-tracer is 4 hours and 21 minutes, with the time lags ranging from less than 1 hour to up to 12 hours. Despite various sources of error such as the low resolution and the additional travel time between the RG front and measuring gauge, the findings are well-paired with the results of the two shown artificial tracer tests. Recharge pulses in the investigation area are caused by rainfall events and/or melting of snow and/or ice.

4.4.2 Flow component separation

Applying Equation 8 to Q vs. EC data shown in the previous section, a rough approximation of the shares of event water with low electric conductivity and pre-event water with increased EC can be made. As input parameters the highest measured EC of 281 µS/cm on the 06.11.2015 issued as the "pre-event water electric conductivity" EC_{old}, while the only rainwater sample from fall 2017 is used as the input parameter EC_p with the value of 42 µS/cm. Since at least some part of the so called "event water" characterized by low residence times, originates from melting ice and snow which are known to have lower EC values as the used rainwater sample, but also the infiltrating water at HK04 and HK05 shows a higher EC (compare Table 6) the presented results of the graphs shown in Figure 28 are somewhat unreliable in their exact values.

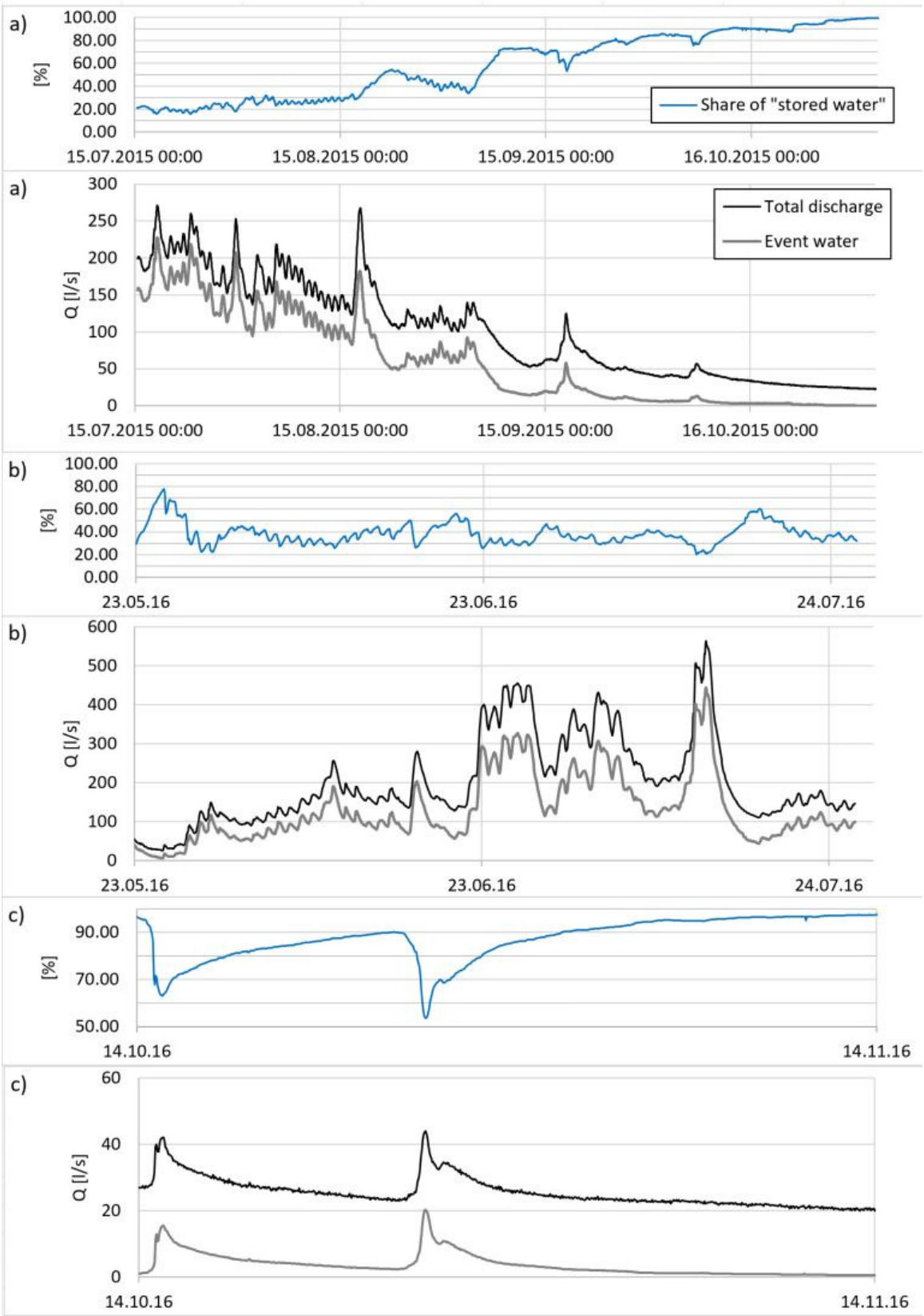

Figure 28: Development of total discharge(black) and the according event water (grey). Blue: share of longer stored, i.e. more TDS enriched, water contributing to the total discharge.

Since the used discharge separation method (Equation 8) relies solely on the EC as a distinction parameter, the overall behavior and trend in Figure 28 is analogue to the description of Figure 26 in the previous section.

During late spring (May and June) when the snowmelt is at its maximum the share of event water increases, until the discharge peak in July, the rock glaciers internal water balance is positive, and the storage is filled. The share of drained pre event water shows daily variations and ranges between 20 and 60 % during this period of high discharge in May, June and July (Figure 28b)). Sudden multiplied discharge values that can occur during this season are at first mainly built up by event water, while post event the share of groundwater is increased above its pre-event level. The hydraulic pulse hits the long-term storage of the rock glacier who is then drained proportionally to the force of the hydraulic pulse.

When the highest discharge is reached, the recession starts and deferred by some precipitation events but nevertheless steadily the share of pre-event water increases while the overall discharge decreases. In Fall (October) the event water share sinks below 5 % in during dry periods (Figure 28 c)). This groundwater dominated season most likely lasts until the next melting season in the following year.

4.4.3 Stable Isotopes

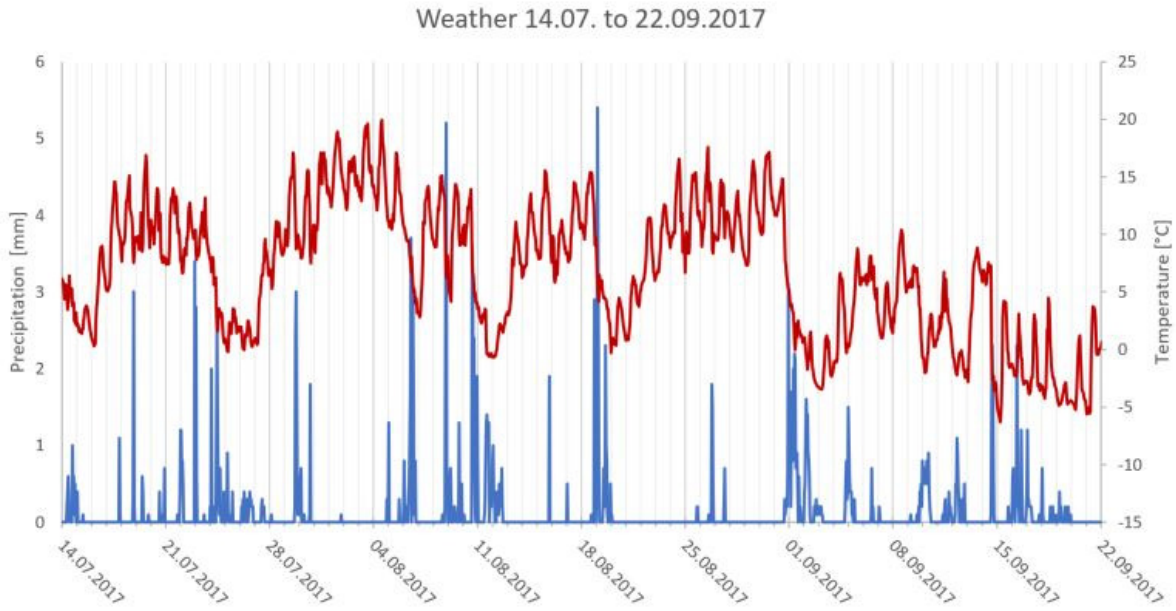

Figure 29: Air temperature and precipitation data during the field days from July to September 2017.

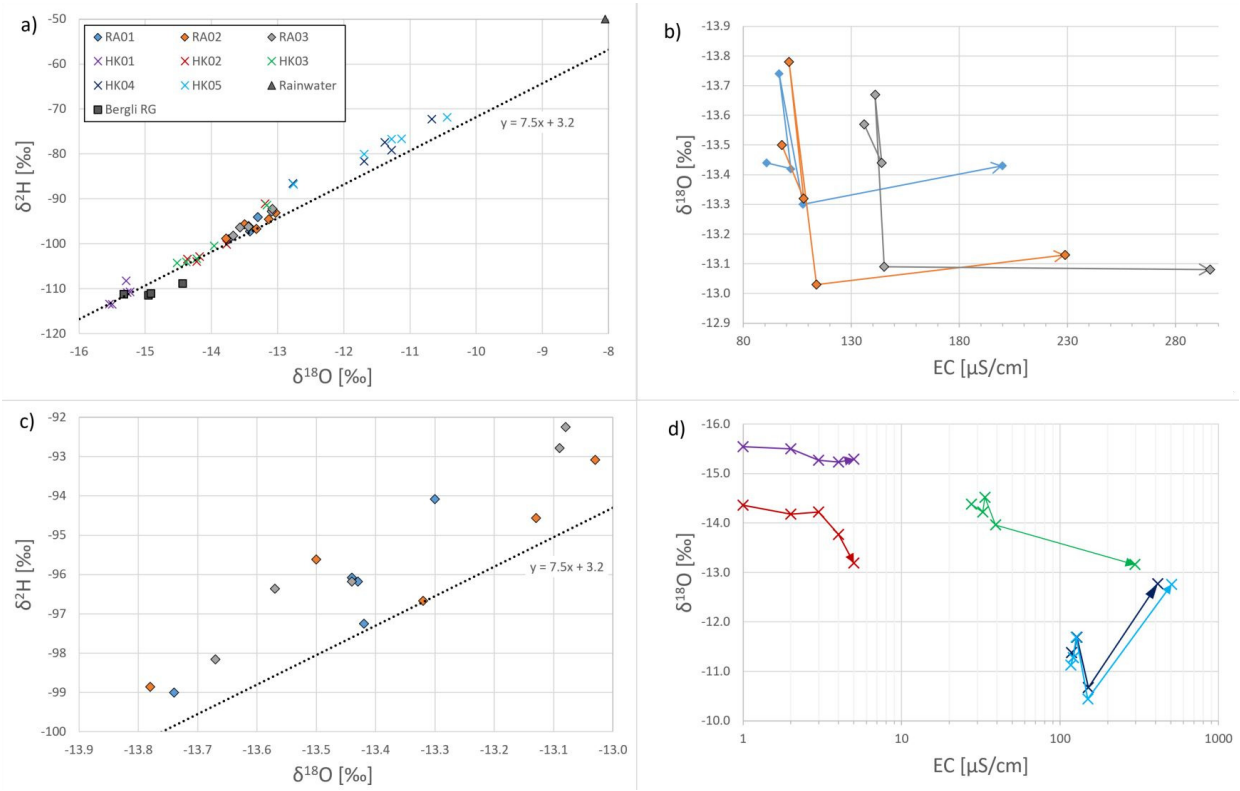

Figure 30: a): Austrian Meteoric Water line (AMWL, y=7.5x+3.2) and gathered isotope data in the research area. For comparison the isotopic signature of ice samples of Bergli RG are plotted as well. Compare with Figure 7 for exact sampling locations at ÖGS RG. b): $\delta^{18}O$ vs. electric conductivity at the spring locations RA01-03, Numbers indicate on which day the samples were taken (1: 01.08. am; 2: 01.08. pm; 3: 02.08.; 4: 10.08.; 5: 15.09.) c): Detailed view on the isotopic signature of RA01-03. d): $\delta^{18}O$ vs. electric conductivity at the sample locations in the catchment area of ÖGS RG, HK01-05.

As visible in Figure 30 a) the gathered isotope data of the rainfall, catchment area and the rock glacier springs aligns with the Austrian Meteoric Water line (AMWL) by Hager et al. (2015), a general shift towards a deuterium excess is reconcilable. As the extrema, the glacier ice sample of HK01 ($\delta^{18}O$= -15.5; $\delta^{2}H$= -113.5) for the lightest and the rain water sample ($\delta^{18}O$= -8.1; $\delta^{2}H$= -50.0) form the two end members of the data span. The samples were taken between the 31.07.2017 and 15.09.2017 in irregular temporal extent which can be seen in Figure 8 With an exception of HK04 and HK05, the sampling locations isotopic data form fairly tight groups with unspecified but little variation. Looking at the isotopic data from the surface waters taken in the catchment area (HK01-05) it can be seen that they follow the meteoric line successive their height above sea level. The highest location HK01 is the strongest depleted while HK04 and HK05 share the lower end of depletion. Interestingly the rock glacier springs (RA01-03) form a rather thigh group (Figure 30 c)). This indicates a close relationship or even a common water origin of the three springs. Instead of individual clusters the sampling locations show a similar spread of their samples along the meteoric water line, the mean value for all three spring locations (RA-) is approx. $\delta^{18}O$= -13.4; $\delta^{2}H$= -95.8. Compared to the overall spread of all samples, the (RA-) spring samples plot approx. in the middle of the catchment areas isotopic span. Since the correlation of height and depletion as set by the HK- sampling locations, is not followed by the rock glacier springs, a mixing with at least a second water source inside the rock glacier itself is suggested. Considering the isotopic signature of the Bergli RG ice samples in this diagram, melted rock glacier ice would be the best guess for this phenomenon. The only rainfall sample gathered from 31.07. to 10.07.2017 plots at a fair distance with a much heavier isotopic signature as all other samples. Given the fact that the rain sample, despite located at the average height of the catchment area, plots well above the HK and RA samples, present rainwater as collected from 31.07 to 10.08.2018 plays only a minor role in the composition of the base runoff. Overall the spring signatures are coherent with previous findings from research on isotopic signatures at ÖGS rock glacier and other active rock glaciers by Krainer et al. (2007).

Figure 30 b) displays the relationship of the $\delta^{18}O$ signature and the electric conductivity. The rock glacier spring samples (RA) are relatively consistent in their EC in August, while showing some variations on the first decimal place in their $\delta^{18}O$ signature. September samples EC however effect a plot further apart, but the $\delta^{18}O$ signature is not influenced by the EC in a distinguishable way. The spread in EC of the three locations indicates that not the entire rock glacier aquifers water is homogenized equally. Generally, high conductivities measured at HK04 and HK05 are not reached by the springs (compare Figure 30 d)), this is another indication for the second RG internal water source. A consistent relationship between EC and $\delta^{18}O$ signature is not visible.

The $\delta^{18}O$ values vs. EC of the samples in the catchment area are shown in Figure 30 d), the samples HK02 and HK03 as well as HK04 and HK05 are practically identical in their value and behavior. This seems reasonable as the sampling locations are close to each other and connected by fast flowing streamlets. HK01 is very stable, the sampling location is a streamlet on top of the bare surface of Hinterer Ölgrubenferner, thus it can be considered as the undisturbed glacier ice signature. This fact is validated by the samples of the 15.09.2018, where all locations but HK01 show a convergence in their $\delta^{18}O$ signature towards approx. 13 ‰ (Figure 30d)). An effect that could be explained with the sudden fall in temperature and snowfall event on the previous days. Thus, the amount of water from the melting glacier Hinterer Ölgrubenferner is significantly lower and the remaining water comes from the vadose zone or groundwater of the moraine and block material.

The samples taken on the 1st and 2nd of august 2018 at temperatures around 10-15 °C and no rainfall (compare Figure 29), show little variation most likely induced by daily discharge variations (Figure 30 d)) On the 1st September 2018 the temperature dropped from +15°C to below 0°C, the beginning of a several week long period with cold weather. Samples taken on 15.09.2018 can therefore be considered ”no recent recharge” samples. The effect is mainly visible in the measured electric conductivity, which are up to 11x (!) higher than the values measured in early august 2018. But the effect is not recorded evenly in all sample locations. While HK01 is constant regarding the EC, the other catchment samples at HK02, HK03, HK04 and HK05 show far higher values than their earlier records. Similarly to the $\delta^{18}O$ signature this time the height corresponds inversely to the measured EC values, the lower the location the higher the EC. Despite the lack of proper discharge measurements due to technical failures in summer 2017, it was clear that the streamlets where the samples were taken carried less water compared to august and were partly frozen.

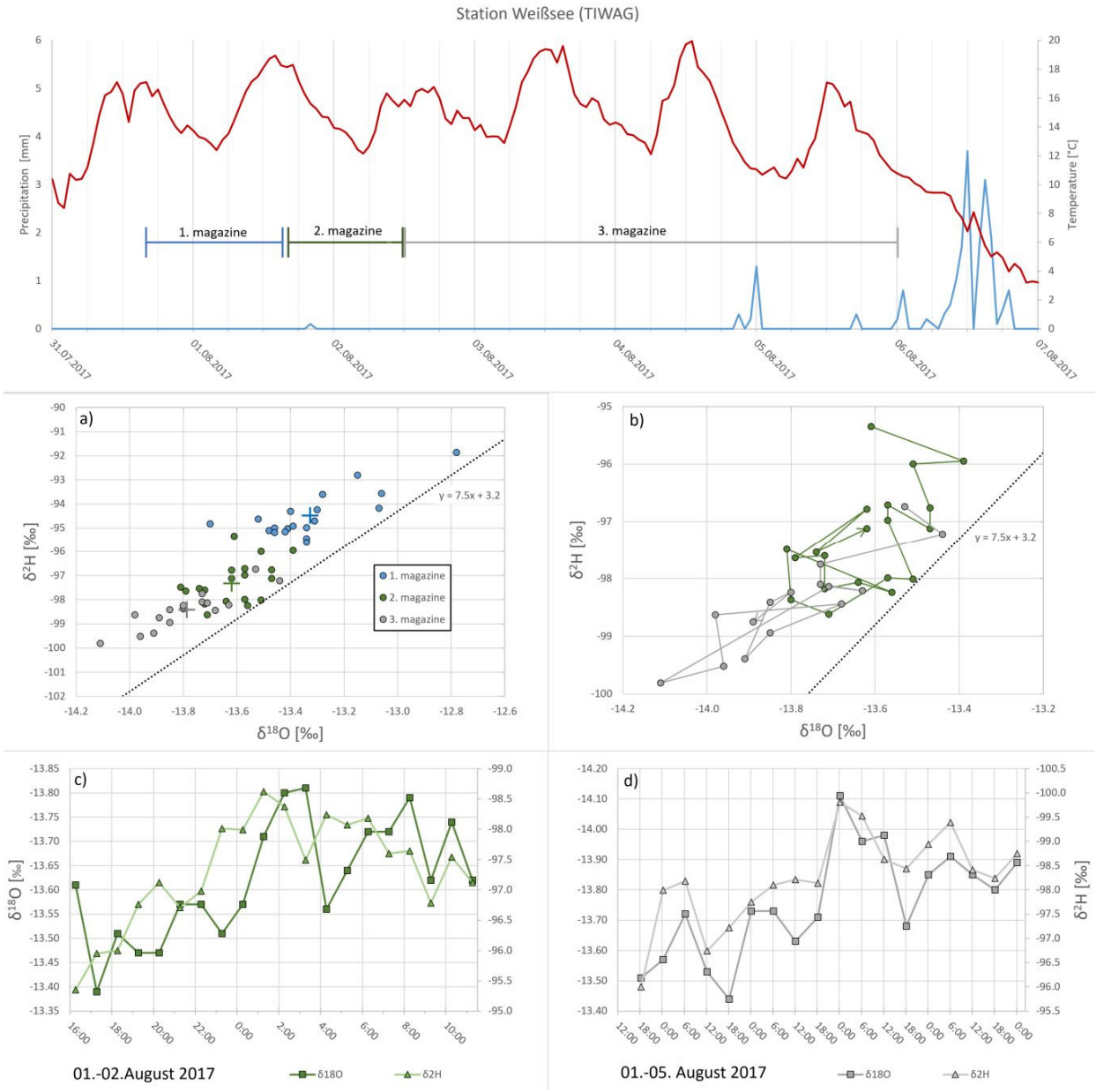

Figure 31: Isotope samples gathered with the automatic sampler device from 31.07.2017 to 06.08.2017 and the corresponding weather record at station Weißsee. The samples are taken at the water gauge and compromise all runoff water of the rock glacier ÖGS. The sampling device holds 24 bottles (=1 magazine) which can be filled automatically before a new magazine has to be inserted. a): Isotope plot of all three magazines along the AMWL (y=7.5x+3.2), the crosses are the mean values of each same colored magazine. b) Detailed view on the successive isotope plot of magazine 2 and 3. c) and d): $\delta^{18}O$ and $\delta^{2}H$ progression of magazine 2. and 3, the first three values in chart d) are taken from magazine 2.

Additionally, to the manually taken samples at the springs and in the catchment area, composite samples of the total runoff were taken at the water gauge location. With the goal of detecting possible daily variations in the isotopic signature an automatic sampling device was set up un the 31.07.2018. The device is equipped with a magazine of 24 bottles, it can be programmed to take samples in each desired interval, for magazine 1 and 2 the interval was set to 1 hour. Unfortunately the first magazine was filled up irregularly so that it can only be said that the samples of magazine 1 were taken between 16:13 o'clock on the 31.07. and 15:18 o clock on the 01.08.2018, but no further succession can be made out. In Figure 31 a) the isotopic data is plotted separated in the three magazines, a trend towards a generally lighter isotopic signature is observable.

The successfully recorded series in magazine 2 (1-hour interval) and magazine 3 (6-hour interval) can be seen in Figure 31 b). Magazine 2 includes 20 samples, the development path leads to a lighter

signature for the first 10 hours, following a backdrop towards the earlier values of this series in the last 10 samples. Considering the third magazines longer sampling interval the behavior of "spiraling" towards a generally lighter isotopic signature is still observable. Based on the data of magazine two, a daily cycle can be observed. A superordinate system then induces the general trend towards lighter isotopic signatures. As recorded by the rain sample (Figure 30) ($\delta^{18}O$= -8.1; $\delta^{2}H$= -50.0) present summer rainfall is expected to have a far heavier isotopic signature. Prior to the field days, in the end of July 2017 the area was hit by rainfall (compare Figure 29) which might have caused an overall heavier isotopic signature, whose degradation is then recorded during the fair weather period in which the main field work and sampling took place.

Figure 31 c) and d) display the separated $\delta^{18}O$ and $\delta^{2}H$ values of each sample of magazine 2 and 3. The general trend is recorded by both the deuterium and oxygen, but the detailed behavior can be opposed to each other. Examples are: from the first to the second sample in Figure 31 c) the trend of $\delta^{18}O$ and $\delta^{2}H$ are contrary to each other, while the oxygen signature gets heavier, the deuterium signature lightens. The effect is also observed with swapped roles, for example around 2 o'clock in the 02.08.2017. At other instances the behavior seems to be aligned, as shown in the last few samples of chart c) and d). The effect is also visible in Figure 31 d), where the sampling interval is 6h with a time span of 4 days (the first 3 samples are taken from magazine 2). From 18:00 to 00:00 the trend is always towards a heavier signature in both elements. Unlike from 06:00 to 12:00 were the trend is aligned on the 02.08. and the 05.08., but crossed on the 03.08. and furthermore swapped on the 04.08.2017.

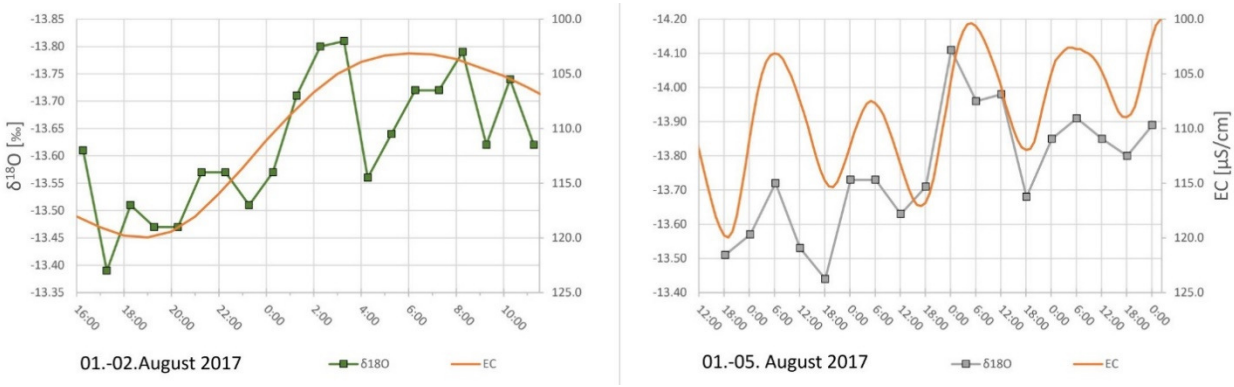

Figure 32: Comparison of the development of isotopic signature and EC in early August 2017. Note: inverted EC axis!

Comparing $\delta^{18}O$ signature and EC from early August 2017 in Figure 32 reveals a possible connection. From 01.08. to 02.08 the EC record shows a typical daily development, the $\delta^{18}O$ signature roughly follows this trend. In the longer but lower resoluted series from 01.-05.08. an alignment of the peaks and valleys of both curves can be noticed.

4.5 Weather and discharge dynamics

Aligned with the temperature and precipitation of the nearby TIWAG weather station “Weißsee” some statements to the discharge dynamics can be made. Figure 33 displays and overview of the most important weather parameters air temperature and precipitation from 01.06.2014 to 12.06.2017. The mean air temperature for all 3 years is 0.68° C, the warmest day was the 07.07.2015 with an average of 16.3° C and the coldest day was the 06.01.2017 with a mean temperature of -22.4° C. The heaviest precipitation in a single day was measured on the 05.08.2016 with 28.9 mm, while the annual average precipitation sum for the years 2013 to 2016 is 642 mm. Comparing the time series in general it can be seen that once the temperature is persistent below the melting point the discharge drastically decreases and shows a less pronounced variability. During the winter month the precipitation comes in form of snow and is thereby stored in the snow blanket until the late spring. In consequence an undisturbed recession of the aquifer is recorded. Early spring rainfall such as the pronounced peak in late April 2015 creates only a damped signal, possibly a still thick consolidated snow planked does not yet allow fast infiltration. Around April each year, the air temperatures increase above 0° C and the snow begins to melt. This leads to the fact that the maximum runoff is usually reached around June due to the combination of the increasing amounts of rainfall and melting snow except the year 2014 were the maximum runoff was reached on 1st of August. The maximum runoff of several 100 l/s does not last longer than a few days, typically the discharge rapidly decreases to values of around 100 l/s to 140 l/s. The trend is gets interfered by new rainfall events but the maximum runoff values caused by late spring snowmelt are not reached until the next year.

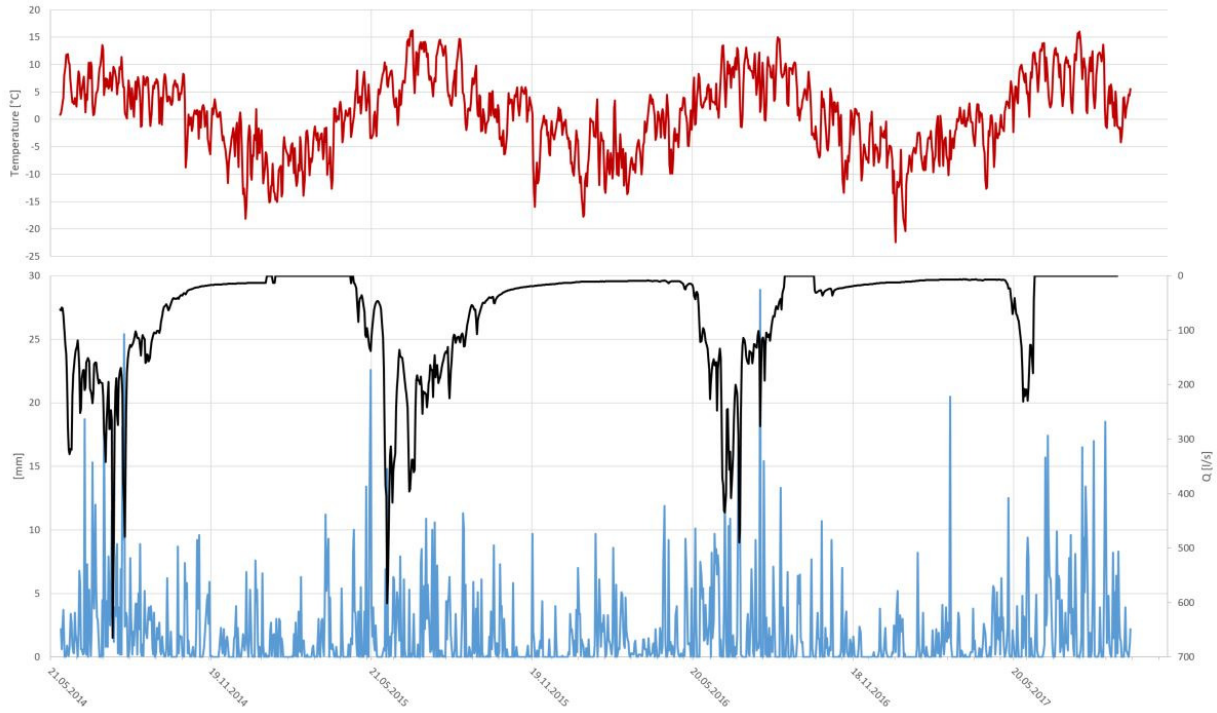

Figure 33: Long term overview of the weather-discharge interaction from 01.06.2014 to 12.06.2017. Temperature and precipitation record at the TIWAG meteorological station "Weißsee". Red: daily average temperature; blue: daily precipitation sum; black: daily average runoff at ÖGS water gauge.

Figure 34 highlights the weather conditions and daily discharge for the period 2015/2016. Clearly visible, the maximum measured runoff (602 l/s) is around the 8th of June 2015, where the snow melt coincides with a precipitation event of up to 15 mm a day. But an even stronger precipitation event around the 20th May 2015 did not nearly cause a similar peak in the discharge record. Here it is

especially visible that temperature works as the main trigger. After the snow melt and the related maximum runoff, the summer rainfall events can cause a rapid growth of discharge, but only long-lasting rainfall events are able to significantly delay the overall recession trend. From October to April the precipitation events are not visible in the runoff record implying that no infiltration takes place during this phase and all precipitation comes as snow. The minimum discharge is reached in late March 2016, before the temperature start to rise again and the first small peaks are recorded in the runoff log.

A detailed insight in the daily temperature and runoff cycles is displayed exemplary in Figure 35. The same time frame as in Figure 21, from 04.08.2016 to 16.08.2016 is shown to further explain the daily range. A rainfall event at the beginning of the time period increases the runoff value by about 70 l/s from about 150 l/s to 220 l/s, the following days are dry and 6 days later the recharge effect is gone. Temperature shows a typical day and night cycle, its rhythm and duration is clearly followed by the runoff with a time lag of about 12 to 14 hours. The ups and downs in the runoff are caused by some sort of melting process because it is linked with the daily temperature variations. Since this takes place in august, were the winter snow is melt and no significant rainfall is measured in this period, only melting ice from the glacier “Hinterer Ölgrubenferner” and/or the active rock glacier itself remain as the root of the daily discharge variations.

The observed dynamic is consistent with previous findings from Berger et al. (2004), Krainer et al, (2002) and especially Rieder (2017) who partly used the same data set as this work.

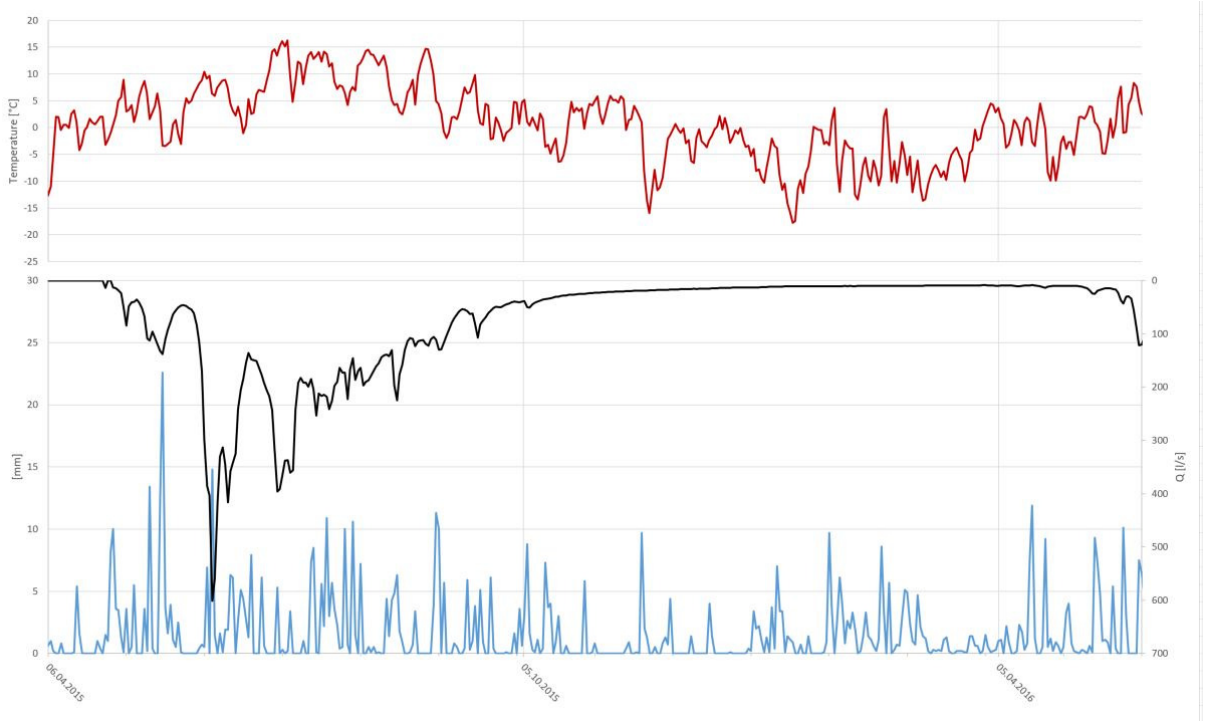

Figure 34: One year long example period 2015/2016. Temperature and precipitation record at the TIWAG meteorological station "Weißsee". Red: daily average temperature; blue: daily precipitation sum; black: daily average runoff at ÖGS water gauge.

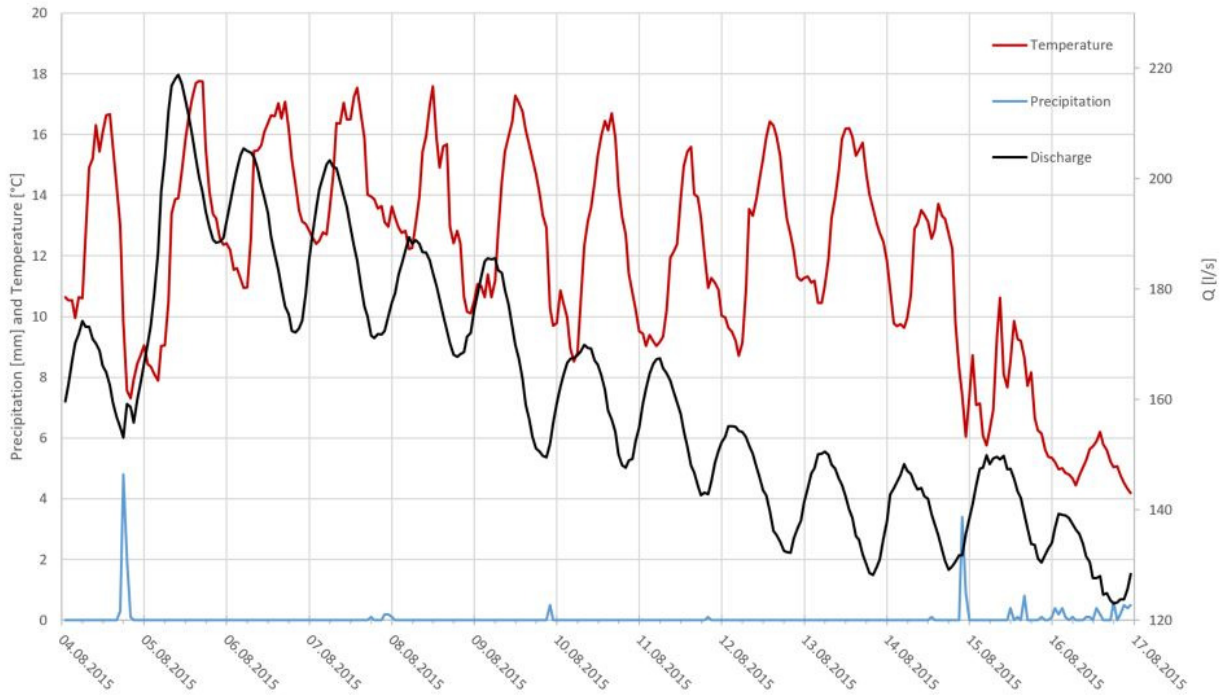

Figure 35: Detailed insight in the daily variations from 04.08.2015 to 16.08.2015. Air Temperature and precipitation record at the TIWAG meteorological station "Weißsee". Red: hourly average temperature; blue: hourly precipitation sum; black: hourly runoff at ÖGS water gauge. The daily temperature and runoff cycles are roughly similar in their duration.

5 Discussion

In general, the new data recorded for this thesis support the existing findings and descriptions of the hydrological dynamics of active rock glaciers, in particular of ÖGS rock glacier (Krainer, et al., 2002, 2007; Berger, et al., 2004; Rieder, 2017).

As a novelty the baseflow is recorded for a whole hydrological year for the season 2015/2016. For 2014/2015 and 2016/2017 despite the record gaps, there is strong evidence regarding the hydrograph that liquid water was discharged over the whole hydrological year. The lowest measured runoff values are in the range of 7 to 13 l/s, but due to the missing calibration measurements and the setup of the gauging station these exact values are quite uncertain. However, the proven winter runoff confirms the findings of Hausmann et al. (2012) who state an ice-free sediment layer at the contact of the rock glacier to the bedrock by geophysical data.

The active rock glacier Ölgrube Süds three major springs are characterized by extreme discharge variability numericized in a discharge quotient (Q_{min}/Q_{max}) of 0.012 to 0.018. These values are regularly estimated for karst springs (e.g.: Goldscheider, et al., 2007) and meanwhile relict rock glacier springs (Winkler et al., 2016) usually indicating aquifer components with low and high storage capacity. The discharge maxima are typically reached during the melting season in early summer, but heavy rainfall can also trigger a strong rise of discharge in the course of a few hours. Sharp runoff peaks are followed by a fast recession component where a major part of the event flow is drained. In the summer when the catchment areas temperatures rise, the discharge is characterized by daily variations in the range of approx. 25 l/s, largely induced by melting of snow and ice from "Hinterer Ölgrubenferner".

The application of the Maillet equation on the recession limbs of the hydrograph via a MRC puts numbers to a three-staged discharge system which is capable of describing the runoff as recorded at the water gauge in "Schiltibach". A fast flow component, draining event water within hours after their accumulation leads to a multi-annual value of α_1= 0.163 d^{-1}. While a rather underdeveloped mid-section of α_2= 0.022 probably depicts the least explored discharge system component, a baseflow with α_3= 0.005 defines the lower end of the recession curve. The spread over more than two orders of magnitude goes well with the very low discharge quotient. The conceptual model, with preferential flow paths on the one side and a water storage with distinct effective porosity on the other side, known from karst landscapes or relict rock glaciers remain adequate. An interaction with rock glaciers internal ice may delay the fast flow and smoothen the transition into the baseflow.

Two artificial tracer tests conducted in 2015 and 2017 are evidence for the existence of a fast lane for infiltrating water. First detection in less than 3 hours and a reached peak concentration in only 4 h 28 min and 5 h 20 min after the injection of the tracer result in a hydraulic conductivity K= 5.3 x 10^{-2} m/s. The 2017 tracer test resulted in a very high recovery rate of >85%. This test confirms the fast component enabling event water to pass through quickly and without significant mixing. A comparison with the slightly slower breakthrough in 2015 alongside the lower recovery rate shows that the flow path is not predetermined, also it could be possible that flow paths change over the years.

Uranine tracer breakthrough times match the average time lag of 4 h 21 min registered by a falling electric conductivity after recharge events induce a hydraulic impulse on the rock glaciers runoff.

Recharge events, namely rainfall and/or melting snow and ice, rapidly cause rising runoff values. The analysis of EC shows that the main part of event water passes through the rock glacier within about 4 hours, thus heavy rainfall or strong and lasting melting events bypass the rock glaciers storage system behaving somewhat like surface runoff. Discharge separation indicates that the runoff spikes are mainly compromised by the event water and the pre-event water share stays fairly stable. There is a factor of uncertainty since melting rock glacier ice and infiltrating event water is hardly distinguishable by their electronic conductivity, thus no statement can be made about the exact influence of melting rock glacier ice on the runoff solely by reviewing the EC record.

As previously suggested in section 4.2, being aware that a major part of the quick event runoff does not interact with the rock glaciers storage system, the volume of stored water can be adjusted by disregarding the volume V_1 that is drained during the first few hours of event runoff.

Table 7: Calculated volumina of stored water disregarding the fastest discharge component. Theoretical aquifer heights adjusted to the lower storage at an assumed porosity of 0.2.

Period:	Stored volume V_{2+3} [x10^6 m^3]	Theoretical aquifer height at porosity 0.2
2014 /2015	0.584	12
2015/2016	0.612	13
2016/2017	0.342	7

The exclusion of the fast flow component at the calculation of the aquifer storage leads to lower volume of overall stored water as shown in Table 7. Interestingly the values of the periods 2014/2015 and 2015/2016 converged to an insignificant difference, while the latest period 2016/2017 falls short by roughly 45 % compared to the earlier periods. The difference might lie in the missing data of the transition period from event dominated discharge to baseflow in the data record of 2016 in a way that the α_2 (V_2) is underestimated. The good coincidence of the first two periods might indicate that this is the rock glaciers true storage and excess water is quickly drained with the fast flow component. A hydrological connection to talus and moraine material is thinkable, which would increase the storage capabilities leading to greater storage capabilities. In conclusion the result of 20 m or less is in the range of the findings from previous research at ÖGS rock glacier. Hausmann et al. (2012) state a 10 – 15 m thick layer of unfrozen sediments which can act as an aquifer.

The applied discharge separation indicates that close to 100% of the baseflow is made up by groundwater. However, true baseflows EC has never been recorded. As an exaggerated example a linear developing descend of the baseflow and linear EC ascend is assumed, at the end of a 180-day recession period EC would be at approximately 350 µS/cm. This value, would lead to significant differences in discharge separation. Applied on the same section a) as in Figure 28 the results are shown in Figure 36.

As an effect the share of groundwater (“stored water”) on the discharge would be further decreased during the event dominated summer season. This shows possible uncertainties in water source shares that must be kept in mind regarding the discharge separation.

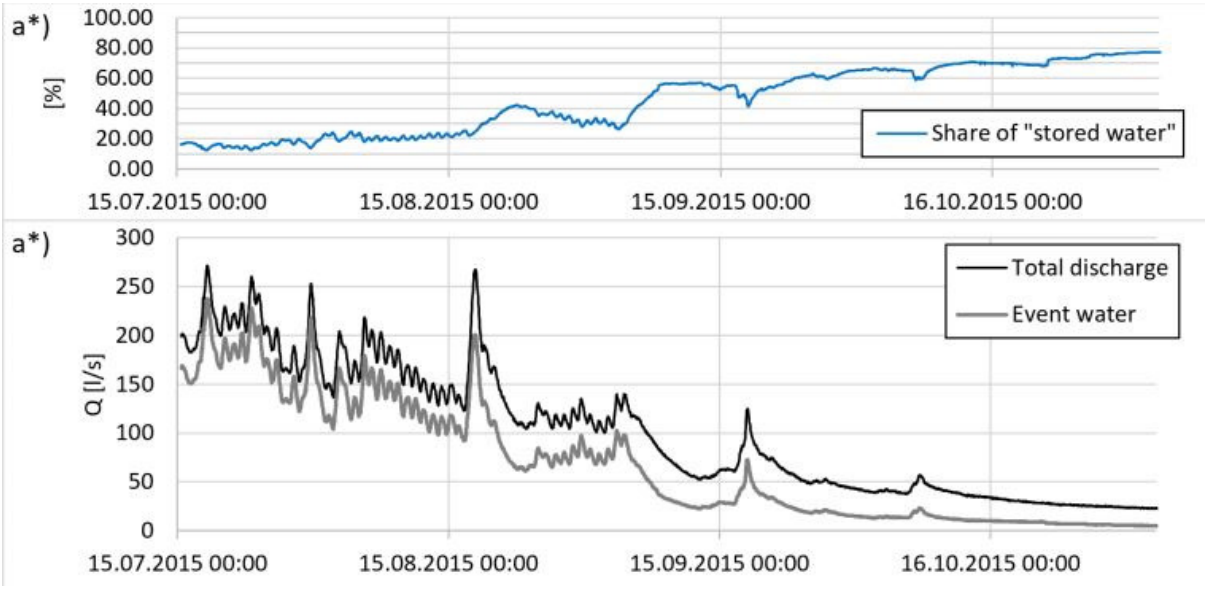

Figure 36: a) Discharge separation based on a theoretical max. EC of 350 µS/cm assumed as the extreme case at the end of a 180-day recession period. Compare to the same section in Figure 28.*

Nevertheless, both discharge separation calculations assume only two water components are mixed, Infiltrating water with lower EC and groundwater with higher EC. But during a field trip on the 15.09.2017 measurements with a handheld current meter showed values up to 505 µS/cm for a rock glacier infiltrating surface streamlet. Stable conditions can be considered for the measurements on the 15.09.2017 as they were conducted after a temperature drop in early September marked the beginning of a weeklong cooling period. Thus measured streamlet water is nearly undisturbed by fresh meteoric waters. Leading to the conclusion, that the lower EC values at the rock glacier springs on that day (200, 229, and 296 µS/cm) are furtherly mixed with a water source inside of the rock glacier. This indicates that a two-component mixing model is not sufficient to describe the ÖGS RG discharge components since rock glacier internal mixing is proven but remains a black box.

Manual EC measurements displayed rising EC values with lower altitude in the catchment area, (compare HK01 to HK05 in Table 6). Since it is shown that melting water from Hinterer Ölgrubenferner causes daily variations at the ÖGS springs, large parts of the melting water cover the distance in a few hours. Since there is no sufficient time for rock-fluid interaction to enrich the melting water in TDS it remains unclear where the rise in EC comes from. But EC measurements done on 15.09.2017 after a temperature drop show that even at location HK02 (glacier mouth) the water is far more conductive than during the fair-weather period (with arguably strong melting) in August. This indicates that groundwater of moraine and talus material is more enriched in TDS (i.e. higher EC). An explanation for the rising EC values with lower altitude is that the share of melting water (low EC, compare HK01) decreases due to an increasing tributary of surface and subsurface water of the talus fans and moraine material with an emerging catchment area. The EC measurements at HK04 and 05 on 15.09.2017 were well above the highest measured EC at the rock glacier springs as well as at the gauge, this indicates rock glacier internal mixing, possibly with melted ice from the rock glaciers core.

Isotopic data supports the thesis of a moraine and talus groundwater contribution, as all samples at HK02 to 05 show a convergence towards approx. $\delta^{18}O$ = -13‰ (Figure 30). Samples on 15.09.17 at HK02 and HK03 are enriched and HK04 and HK05 are depleted, compared to their earlier samples, indicating a common water source (groundwater).

As already broached in chapter 4.4.3 “stable isotopes” the height - depletion trend set up by the isotopic signature of the surface waters sampled in the rock glaciers catchment area is broken by the spring water samples. A comparison with rock glacier ice samples from Bergli rock glacier or the quasi glacier ice samples HK01 of Hinterer Ölgrubenferner, indicates that the missing mixing component is most likely rock glacier internal ice.

The isotope data series from 01.-05.August follows a trend from heavier- towards lighter isotopic signatures, i.e. decreasing share of rainwater towards increasing share of melted ice (Figure 30 and Figure 31). Plotted in a EC vs. $\delta^{18}O$ diagram a somewhat spiraling trend is pictured (Figure 37). Additionally, three samples showing the measured extrema are displayed. For the ice sample the mean of HK01 is used, being the least conductive and most depleted in $\delta^{18}O$. The Rain sample is the least depleted in $\delta^{18}O$, i.e. heaviest isotope sample. The HK05 sample from 15.09.2017 is thought to come nearest to the true groundwater due to its maximum conductivity, and the previously described $\delta^{18}O$ signature (keyword: convergence).

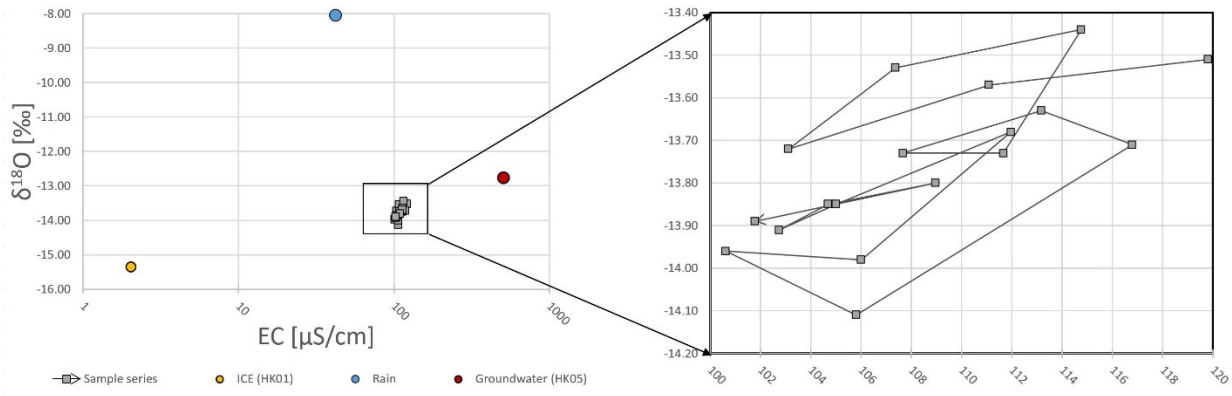

Figure 37: Mixing diagram of EC and $\delta^{18}O$ of stream water samples taken in 6-hour intervals from 01.08 to 05.08.2017. For comparison pure glacier ice (HK01), the rain sample and the infiltrating groundwater are plotted.

Spiraling as displayed in Figure 37 is possibly caused by the impact of two discharge systems on the spring discharge. Daily variations (compare Figure 32) can be seen in both EC and isotope data, causing a back and forth development between “groundwater” (HK05) and melted water (HK01). Daily cycles are overlain by a general trend towards an increased share of melting water. As displayed in Figure 31, weather data supports this consideration: in early August 2017 rainfall is negligible and temperatures are well above the melting point. These two developments likely cause the spiraling effect. Since ice- and groundwater sample were taken above the rock glacier their general validity as end members is unsure, rock glacier ice and groundwater remain as the unknown factors of influence.

Summing up, the hydrodynamic of ÖGS rock glacier is the result of several cycles, of whom daily and yearly variations and trends are recurring in a predictable way. The major determinant for discharge variations is the weather situation. It is proven that the discharge system consists of at least two major components, on one hand, fast flow paths cause a karst like behavior of the springs draining a significant part of the yearly recharge with negligible retention times. In general retention capabilities during strong recharge events is very limited. On the other hand, all year long discharge (baseflow), i.e. a permafrost free storage, is proven. Isotope signatures and electronic conductivity measurements suggest already long retention times in the pore volume of moraine material. The effects of rock glacier internal ice and groundwater are shown but without distinct samples their effects can’t be numbered. Findings show that the rock glacier cannot be viewed as an individual system but needs to be seen as the funnel of all the catchment areas hydrological systems.

6 Prospect

The results complement the previous research on active rock glaciers. A karst like discharge behavior is apparent and retention capabilities are limited. Because rock glacier ÖGS is well researched, continuation could enhance its status as a main example of active rock glaciers.

The next step could be the calculation of water balance to unveil the storage capabilities of the catchment area. Then comparison with the relict Ölgrube Nord rock glacier could uncover the influence of the rock glacier internal ice on the storage capabilities.

Alpine environment and limited access during the winter season cause some uncertainties. As the discharge measurements are the backbone of hydrologic research beside a reliable water gauge, reference measurements could be done during peak discharge in early summer and baseflow at the beginning of winter.

Isotopic data in times of peak- and baseflow as well as during and shortly after rainfall could further describe the impact of recharge events on the slow discharge system.

7 Literature

Barnett, T.P., Adam, J.C. and Lettenmaier, D.P. 2005. Potential impacts of a warming climate on water availability in snow-dominated regions. *nature.* 2005, 438, pp. 303-309.

Barsch, D. 1996. *Rockglaciers. Indicators for the Present and Former Geoecology in High Mountain Environments,.* Berling : Springer Verlag, 1996. p. 331.

Berger, Jana, Krainer, Karl and Mostler, Wolfram. 2004. Dynamics of an active rock glacier (Ötztal Alps, Austria). *Quaternary Research.* 2004, 63, pp. 233-242.

Birk, Steffen, Liedl, Rudolf and Sauter, Martin. 2004. Identification of localised recharge and conduit flow by combined analysis of hydraulic and physico-chemical spring respones (Urenbrunnen, SW-Germany). *Journal of Hydrology.* 2004, Vol. 286, pp. 179-193.

Clark, Ian and Fritz, Peter. 1997. *Environmental Isotopes in Hydrogeology.* New York : CRC Press, 1997.

Clark, Ian. 2015. *Groundwater Geochemistry and Isotopes.* New York : CRC Press, 2015.

Clow, D.W., et al. 2003. Ground water occurence and contributions to streamflow in an alpine catchment, Colorado Front Range. *Groundwater.* 2003, 41/7, pp. 937-950.

Dewandel, B. , et al. 2003. Evaluation of aquifer thickness by analysing recession hydrographs. Application to the Oman ophiolite hard-rock aquifer. *Journal of Hydrology.* 2003, Vol. 274, pp. 248-269.

Engel, Michael, et al. 2016. Identifying run-off contributions during melt-induced run-off events in a glacierized alpine catchment. *Hydrological Processes.* 2016, 30, pp. 343-364.

Gödel, S. 1993. Geohydrologie der Blockgletscher im Hochreichart-Gebiet (Seckauer Tauern, Steiermark) [Hydrogeology of rock glaciers in the Hochreichart area (Seckauer Tauern Range, Styria)]. [ed.] University of Vienna. *MSc Thesis.* 1993.

Goldscheider, Nico and Drew, David. 2007. *Methods in karst hydrology.* Leiden : Taylor & Francis, 2007.

Hager, Benedikt and Foelsche, Ulrich. 2015. Stable isotope composition of precipitation in Austria. *Austrian Journal of Earth Sciences.* 2015, 108/2, pp. 2-13.

Hausmann, Helmut, et al. 2012. Internal structure, ice content and dynamics of Ölgrube and Kaiserberg rock glaciers (Ötztal Alps, Austria) determined from geophysical surveys. *Austrian Journal of Earth sciences.* 2012, Vol. 105/2, pp. 12-31.

Hoinkes, G. and Thöni, M. 1993. Evolution of the Ötztal-Stubai, Scarl-Campo and Ulten basement units. [book auth.] J.F. von Raumer and F. Neubauer. *Pre-Mesozoic Geology in the Alps.* s.l. : Springer Verlag, 1993, pp. 485-494.

Hölting, Bernward and Coldewey, Wilhelm G. 2013. *Hydrogeologie, Einführung in die Allgemeine und Angewandte Hydrogeologie.* Heidelberg : Springer, 2013.

Hughes, P.D., Gibbard, P.L. and Woodward, J.C. 2003. Relict rock glaciers as indicators of Mediterranean palaeoclimate during the Last GLacial Maximum (Late Würmian) in northwest Greece. *Journal of Quaternary Science.* 2003, 18(5), pp. 431 - 440.

Kovács, Attila, et al. 2005. A quantitative method for the characterisation of karst aquifers based on spring hydrograph analysis. *Journal of Hydrology.* 2005, Vol. 303, pp. 152-164.

Krainer, Karl and Mostler, Wolfram. 2006. Flow velocities of active rock glaciers in the austrian alps. *Geografiska Annaler.* 2006, 88, pp. 267-280.

—. 2002. Hydrology of Active Rock Glaciers: Examples from the Austrian Alps. *Arctic, Antarctic and Alpine Research.* 2002, Vol. 34, 2, pp. 142-149.

—. 2000. Reichenkar Rock Glacier: A Glacier Derived Debris-Ice System in the Western Stubai Alps, Austria. *Permafrost and Periglacial Processes.* 2000, 11, pp. 267-275.

Krainer, Karl and Ribis, Markus. 2012. A Rock Glacier Inventory of the Tyrolean Alps (Austria). *Austrian Journal of Earth Sciences.* 2012, 105/2, pp. 32 - 47.

—. 2009. Blockgletscher und ihre hydrogeologische Bedeutung im Hochgebirge. *Mitteillungsblatt des Hydrographischen Dienstes in Österreich.* 2009, 86, pp. 65 - 78.

Krainer, Karl. 2015. Blockgletscher in den Ötztaler und Stubaier Alpen: Eine Übersicht. [book auth.] Nikolaus Schallhart and Brigitta Erschbamer. [ed.] Alpine Forschungsstelle Obergurgl. *Forschung am Blockgletscher, Methoden und Ergebnisse.* Innsbruck : Innsbruck University Press, 2015, Vol. 4, 2, p. 198.

—. 2015. Blockgletscher: Einführung. [book auth.] Nikolaus Schallhart and Brigitta Erschbamer. [ed.] Alpine Forschungsstelle Obergurgl. *Forschung an Blockgletscher, Methoden und Ergebnisse.* s.l. : innsbruck university press, 2015, Vol. 4.

Krainer, Karl, et al. 2015. A 10,300-year-old permafrost core from the active rock glacier Lazaun, southern Ötztal Alps (South Tyrol, northern Italy). *Quaternary Research.* 2015, 83, pp. 324-335.

Krainer, Karl, Mostler, Wolfram and Spötl, Christoph. 2007. Discharge from active rock glaciers, Austrian Alps: a stable isotope approach. [ed.] Österreichische Geologische Gesellschaft. *Austrian Journal of Earth Sciences.* 2007, 100, pp. 102-112.

Kresic, Neven. 2007. *Hydrogeology and Groundwater Modeling.* 2. Bocta Raton : CRC Press, 2007.

Kuhn, Michael, Dreiseitl, Ekkehard and Emprechtinger, Markus. 2013. Temperatur und Niederschlag an der Wetterstation Obergurgl, 1953-2011. [book auth.] Eva-Maria Koch and Brigitta Erschbamer. *Klima, Wetter, Gletscher im Wandel.* Innsbruck : innsbruck university press, 2013.

Leibundgut, Christian, Malozewski, Piotr and Külls, Christoph. 2009. *Tracers in Hydrogeology.* Chichester : Wiley-Blackwell, 2009.

Maillet, E. 1905. *Méchanique et physique du globe. Essais d'hydraulique souterraine et fluviale [Mechanics and physiques of the world: an essay of subterranean and fluvatile hydraulics].* Paris : A. Hermann, 1905.

Mook, W.G. 2001. *Environmental isotopes in the hydrological cylce, Principles and applications.* Paris : UNESCO, 2001.

Morgenschweis, G and Nusch, E. 1991. Fliesszeitmessung in der Ruhr bei Niedrigwasserabfluss. Ruhrwassermenge 1990. [ed.] Ruhrverband. *Ruhrwassermenge 1990.* 1991, pp. 38-55.

Morgenschweis, G. 2010. *Hydrometrie, Theorie und Praxis der Durchflussmessung in offenen Gerinnen.* Heidelberg : Springer, 2010.

Mortimer, Charles E. and Müller, Ulrich. 2010. *Chemie.* 10. Stuttgart : Georg Thieme Verlag KG, 2010.

Nyenhuis, Michael. 2005. *Permafrost und Sedimenthaushalt in einem alpinen Geosystem.* [Dissertation] Bonn : ULB Bonn, 2005.

Pauritsch, Marcus. 2016. *Hydrogeologie reliktischer Blockgletscher (Niedere Tauern, Österreich).* Graz : s.n., 2016.

Pauritsch, Marcus, et al. 2017. Investigating groundwater flow components in an Alpine relict rock glacier (Austria) using a numerical model. *Hydrogeology Journal.* 2017, Vol. 25, pp. 371-383.

Posavec, Kristijan, et al. 2017. Method and Excel VBA Algorithm for Modelin Master Recession Curve Using Trigonometry Approach. [ed.] National Ground Water Association. *Groundwater.* 2017, Vol. 55, 6, pp. 891-898.

Rieder, Aaron. 2017. *Geologische, geomorphologische und hydrogeologische Untersuchungen im Bereich Ölgrube, Kaunergrat, Ötztaler Alpen.* Innsbruck : s.n., 2017. unveröff. MA.

Schmid, S.M., et al. 2004. Tectonic map and overall architecture of the Alpine orogen. *Eclogae Geologicae Helvetiae.* 2004, pp. 93-117.

Wels, C., Cornett, R.J. and Lazarete, B.D. 1991. Hydrograph separation: a comparison of geochemical and isotopic tracers. *Hydrological Journal.* 1991, Vol. 122, pp. 253-274.

Winkler, Gerfried, et al. 2016. Identification and assessment of groundwater flow and storage components of the relict Schöneben Rock Glacer, Niedere Tauern Ragne, Eastern Alps, (Austria). *Hydrogeology Journal.* 2016, Vol. 24.

Winkler, Gerfried, et al. 2016. *Reliktische Blockgletscher als Grundwasserpeicher in alpinen Einzugsgebieten der Niederen Tauern.* Graz : s.n., 2016. p. 134, Berichte der Wasserwirtschaftlichen Planung Steiermark.